ENCAPSULATION OF MENTHOL WITH PEG6000 BY RAPID EXPANSION OF
SUPERCRITICAL CARBON DIOXIDE

Mr.Nara   Suankaew

A Thesis Submitted in Partial Fulfillment of the Requirements
for the Degree of Mater of Engineering Program in Chemical Engineering
Department of Chemical Engineering
Faculty of Engineering
Chulalongkorn University
Academic Year 2011
Copyright of Chulalongkorn University

การเคลือบอนุภาคของเมนทอลด้วยพอลิเอททิลีนไกลคอล 6000 ด้วยการขยายตัวอย่างรวดเร็วของคาร์บอนไดออกไซด์เหนือวิกฤต

นายนรา สวนแก้ว

Thesis Title	ENCAPSULATION OF MENTHOL WITH PEG6000
	BY RAPID EXPANSION OF SUPERCRITICAL
	CARBON DIOXIDE
By	Mr. Nara Suankaew
Field of study	Chemical Engineering
Thesis Advisor	Associate Professor Tawatchai Charinpanitkul, D.Eng.
Thesis Co-advisor	Apinan Soottitantawat, D.Eng.

Accepted by the Faculty of Engineering, Chulalongkorn University in Partial Fulfillment of the Requirements for a Master's Degree

………………………..… Dean of the Faculty of Engineering
(Associate Professor Boonsom Lerdhirunwong, Dr.Ing.)

THESIS COMMITTEE

....Chairman
(Associate Professor Ura Panchareon, D.Eng.,Sc.D)

....Thesis Advisor
(Associate Professor Tawatchai Charinpanitkul, D.Eng.)

....Thesis Co-advisor
(Apinan Soottitantawat, D.Eng.)

....Examiner
(Assistant Professor Varong Pavarajarn, Ph.D.)

....External Examiner
(Issara Sramala, Ph.D.)

นรา สวนแก้ว : การเคลือบอนุภาคของเมนทอลด้วยพอลิเอททิลีนไกลคอล 6000 ด้วยการขยายตัวอย่างรวดเร็วของคาร์บอนไดออกไซด์วิกฤต (ENCAPSULATION OF MENTHOL WITH PEG6000 BY RAPID EXPANSION OF SUPERCRITICAL CARBON DIOXIDE) อ. ที่ปรึกษาวิทยานิพนธ์หลัก : รศ.ดร. ธวัชชัย ชรินพาณิชกุล, อ. ที่ปรึกษาวิทยานิพนธ์ร่วม : ดร. อภินันท์ สุทธิธารธวัช, 104 หน้า.

กระบวนการเคลือบหรือผลิตยาที่ทำให้ได้อนุภาคของยาในขนาดซับไมครอนหรือนาโนเมตรเป็นการเพิ่มคุณค่าของผลิตภัณฑ์ยาในอุตสาหกรรมและยังเป็นการปรับปรุงคุณสมบัติที่ผิวให้เหมาะสมกับอวัยวะเป้าหมาย ได้แก่ ความสามารถในการปลดปล่อยฤทธิ์ยาด้วยกลไกการแพร่ผ่านชั้น เป็นต้น ซึ่งกระบวนการผลิตที่ใช้อยู่ในปัจจุบัน เช่น การทำแห้งด้วยการพ่นสเปรย์ การทำอีมัลชัน และอื่นๆ มักมีปัญหาการปนเปื้อนของตัวทำละลายหรือการสลายตัวของยาขณะกระบวนการผลิตเนื่องจากอุณหภูมิที่ใช้ในกระบวนการผลิตที่มีค่าสูง ดังนั้นการพัฒนาให้ได้กระบวนการผลิต/เคลือบยาที่จะทำให้ผลิตภัณฑ์ยาปราศจากตัวทำละลายและมีอนุภาคขนาดเล็กมากที่สุด

กระบวนการผลิต/เคลือบยาโดยของไหลเหนือวิกฤตจึงได้ถูกพัฒนาขึ้น โดยมีแนวคิดใช้สภาวะวิกฤตของสสาร เพื่อเปลี่ยนแปลงคุณสมบัติทางกายภาพของสาร (ยา สารเคลือบยาและตัวทำละลาย) นั้น จากนั้นก็เปลี่ยนแปลงสภาวะของสสารนั้นกลับสู่สภาวะปกติ ได้ผลิตภัณฑ์ยาออกมา โดยหนึ่งในเทคนิคของไหลเหนือวิกฤตที่นิยมใช้ในกระบวนการผลิตยา คือ เทคนิคการขยายตัวอย่างรวดเร็วของสารละลายเหนือวิกฤต เมื่อสาร (ยา สารเคลือบยาและตัวทำละลาย) อยู่ในสภาวะวิกฤตแล้วถูกส่งผ่านหัวฉีดที่มีขนาดเล็ก การเปลี่ยนแปลงทางกายภาพของสารจากสภาวะวิกฤตสู่สภาวะปกติส่งผลให้สารละลายเกิดการอิ่มตัวอย่างยิ่งยวด จากนั้นก็จะเกิดการตกผลึกเป็นอนุภาคขนาดเล็กโดยที่ระหว่างกระบวนการตกผลึกนั้นตัวทำละลายที่ใช้ก็จะเกิดการแพร่ออกจากสารละลายไปพร้อมกัน เทคนิคนี้สามารถใช้กับสารที่มีการสลายตัวของสารที่อุณหภูมิต่ำได้ เช่น เมนทอล ซึ่งใช้เป็นอนุภาคจำลองของยาและพอลิเอทธิลีนไกลคอล 6000 ถูกใช้เป็นอนุภาคจำลองของวัสดุเคลือบผิว พบว่าอนุภาคที่ได้มีขนาด 0.5 ถึง 60 ไมครอน โดยเตรียมสารละลายของเมนทอลและพอลิอิทธิลีนไกลคอล 6000 ในตัวทำละลายเหนือวิกฤตของคาร์บอนไดออกไซด์และเอทานอลที่ความดันในช่วง 100,150,200 บรรยากาศ และอุณหภูมิ 30,40,50,60 องศาเซลเซียส และความเข้มข้นของเอทานอลระหว่าง 0 ถึง 30 เปอร์เซ็นต์โดยน้ำหนัก พบว่าปัจจัยในกระบวนการอันได้แก่ อุณหภูมิก่อนการขยายตัว, ความดันก่อนการขยายตัว และปริมาณเอทานอลส่งผลต่อขนาดอนุภาค การกระจายตัวของขนาดอนุภาค ตลอดจนรูปร่างของอนุภาค

ภาควิชา: วิศวกรรมเคมี ลายมือชื่อนิสิต ....

สาขาวิชา: วิศวกรรมเคมี ลายมือชื่อ อ.ที่ปรึกษาวิทยานิพนธ์หลัก ....

ปีการศึกษา: 2554 ลายมือชื่อ อ.ที่ปรึกษาวิทยานิพนธ์ร่วม ....

4970780221 : MAJOR CHEMICAL ENGINEERING

KEYWORDS : ENCAPSULATION / MENTHOL / SUPERCRITICAL CARBON DIOXIDE

NARA SUANKAEW: ENCAPSULATION OF MENTHOL WITH PEG6000 BY RAPID EXPANDSION OF SUPERCRITICAL CARBON DIOXIDE. ADVISOR : ASSOC. PROF. TAWATCHAI CHARINPANITKUL, D.Eng., CO-ADVISOR : APINAN SOOTTITANTAWAT, D.Eng., 104 pp.

Methods for producing drug particles in the sub-micrometer or nanometer range are one option for enhancing the therapeutic effectiveness of a drug. The using of polymers as a drug coating material widespread in pharmaceutical production for surface modification because it can help improve the circulation and controlled release of the drug in the blood vessels. However, with drug coating/production by conventional methods, such as spray drying and emulsion techniques, high temperature treating could lead to the degradation of the drug.

Supercritical fluid techniques have been developed to produce fine drug particles to overcome the problem. The drug (solute) is first dissolved in the supercritical fluid. Subsequently, the solution is rapidly expanded and depressurized through a nozzle, leading to supersaturation of the solution and the consequent precipitation of solid products with free solvent. This technique could be used with low temperature decomposition substances. In this research, menthol represents the drug and polyethylene glycol with molecular weight 6,000 (PEG6000) was used as the coating material, with the effects of RESS parameters be being investigated.

The experimental results revealed that the obtained menthol particles exhibited a nominal size in a range of 0.5 to 60 micron with pressure in a range of 10 - 20 MPa, temperature in a range of 303 - 333 K and ethanol concentration in a range of 0 – 30 wt%. The RESS parameters which were pre-expansion temperature and pre-expansion pressure affected morphology, particle size and particle size distribution. It was also found that ethanol could help control morphology, particle size and particle size distribution.

Department : __Chemical Engineering__ Student's Signature ....

Field of Study : __Chemical Engineering__ Advisor's Signature ....

Academic Year : _2011_....................... Co-advisor's Signature ....

ACKNOWLEDGEMENTS

CONTENTS

CHAPTER   Page

LIST OF TABLES

LIST OF FIGURES

Page

Page

Page

Appendix A

NOMENCLATURES

C_p	Heat capacity
EOS	Equation of state
FDA	United state Food and Drug Administration
FT-IR	Fourier transform infrared spectrometer
F-S	Fluid-solid boundary
f	Fugacity
H	Enthalpy
G	Gibbs-free energy
GAS	Gas antisolvent process
k	interaction parameter
L-L	Liquid-Liquid boundary
OM	Optical microscope
P_c	Critical pressure
PEG6000	Poly(ethylene glycol) with molecular weight 6000
P_{pre}	Pre-expanson pressure
PR	Peng-Robinson equation of state
PSD	Particle size distribution
r	Size parameter
R	Gas constant
RESS	Rapid expansion of supercritical solution
S	Degree of saturation
SAS	Supercritical antisolvent process
SCF	Supercritical fluid
SC-CO$_2$	Supercritical carbon dioxide
SEM	Scanning electron microscope
SRK	Soave-Redlich-Kwong equation of state
S-L	Sanchez-Lacombe Equation
T_c	Critical temperature

TGA	Thermogravimetric
T_{pre}	Pre-expansion temperature
w	mass fraction
wt	Weight
x	Molefraction in liquid phase
y	Mole fraction in gas phase
α	Coefficient of thermal expansion
φ	Fufacity coeffiecient
Φ	Close pack volume fraction
ρ	Density
ρ_c	Critical density
μ_{JT}	Joule-Thomson coefficient
π^*	Dipolarity/polarizabilit; solvent strength parameter

Subscript

eq	Equilibrium
Eq	Equation
*	Characteristic
~	Reduced

CHAPTER I

INTRODUCTION

1.1 Background and motivation

Recently, the development of pharmaceutical and cosmetic industrial sectors have paid more attentions on high quality products therefore many researchers have proposed new ideas to apply nanotechnology in pharmaceutical and cosmetic processes. Such technology could provide very fine particles of active substance encapsulated with coating material in range of nanometer or micrometer for the purpose of the surface modification with a function of controlled-release.

In general aim of encapsulation is to adjust surface properties of core particles for applications of drug delivery. Therefore, many surface properties which are pH, biocompatibility, ability of controlled-release have become issues of drug production.

There are many techniques for encapsulation, e.g. spray drying and emulsion. These conventional techniques are hard to avoid using high temperature during operation and organic solvent that is difficult to remove it clearly. Thus all these drawbacks have already motivated chemical engineers and chemists in pharmaceutical industries to look for new and cleaner solvents.

In past decades, the use of supercritical fluids (SCF), one of promising alternatives has been recognized. There are many techniques of supercritical fluids such as rapid expansion supercritical solutions (RESS), gas anti-solvent process (GAS), supercritical anti-solvent process (SAS) etc. However, the RESS process is recognized as the simplest one. It has been employed to encapsulate particle of active substance with polymers in case that both materials can be dissolved in supercritical fluid.

For the RESS process, the controlled size and morphology of composite particles, would be affected by many parameters that we have to concern such as chemical structure of substance and RESS parameters (pre-expansion temperature; T_{pre}, pre-expansion pressure; P_{pre}).

In this research, the author set an objective to prepare composite particle of an active substance (menthol) and coating material (PEG6000). Then some operating which are pressure, temperature and ethanol concentration will be varied for examining their effects on the properties of encapsulated products.

1.2 Objective of the research

The prime objective of this research was obtaining the fundamental knowledge about the controlling of morphology, particle size, particle size distribution in order to apply such the knowledge to produce micronized menthol, micronized PEG6000 and formation of the composite between menthol and PEG6000.

1.3 Scope of research

1.3.1 Formulate micronization of menthol by using rapid expansion of supercritical carbon dioxide under the designated conditions; pre-expansion temperature at 303, 313 and 323 K; pre-expansion pressure at 10 MPa, 15 MPa, 20 MPa; ethanol concentration at none, 10 wt%, 30 wt%. and then investigate the effect of RESS parameter.

1.3.2 Formulate micronization of PEG6000 by using rapid expansion of supercritical carbon dioxide under the designated conditions; pre-expansion temperature at 313 and 323 K; pre-expansion pressure at 15 MPa, 20 MPa; ethanol concentration at 10 wt%, 30 wt%. and then investigate the effect of RESS parameter.

1.3.3 Formulate the composites of menthol and PEG6000 by using rapid expansion of supercritical carbon dioxide under the designated conditions pre-expansion temperature at 313 and 323 K; pre-expansion pressure at 15 MPa and 20 MPa; ethanol concentration 10 wt% and 30 wt%. and then investigate the effect of RESS parameter.

Characterize the obtained particles by following instruments:

- Optical Microscope (OM)
- Scanning Electron Microscope (SEM)
- Thermogravimetric Analysis (TGA)
- Fourier Transform Infrared Spectrophotometer (FT-IR)

1.4 Procedure of the research

1. Conduct literature survey and review.

2. Establish experimental set up (Chemicals and apparatus).

3. Carry out preparation and characterization of menthol particle.

4. Carry out preparation and characterization of PEG6000 particle.

5. Carry out preparation and characterization of menthol/PEG6000 composite particle.

6. Characterize the obtained products by the above instrument.

7. Wrap up or do more experiments if necessary.

8. Write thesis and prepare draft manuscript for journal publication.

1.5 Benefits obtained from this work

1.5.1 Fundamental knowledge related to the encapsulated particles and controlling particle size, particle size distribution and morphology of the product by using rapid expansion of supercritical carbon dioxide has been examine.

1.5.2 Knowledge to control the particle size, particle size distribution and morphology with gain good quality of the product has been examined.

CHAPTER II

FUNDAMENTAL KNOWLEDGE AND LITERATURE REVIEW

2.1 Rapid expansion of supercritical solutions (RESS)

This process is used when the polymer has a low degree of solubility in normal condition. The polymer is generally dissolved in a supercritical fluid when a high-pressure solution is rapidly depressurized through an adequate nozzle, and a result polymer precipitation occur at low pressure. The process is based on the solubility difference at high and low pressures. The principle governing pressure-induced phase separation is illustrated in **Figure 2.1** . Along with the pressure quench, the solution experiences a temperature quench as shown in **Figure 2.2.** Depending upon the process temperature, as well as the glass and/or the melting transition temperature of the polymer and the degree to which these transitions may have been lowered, and the path followed from the homogeneous one-phase region, the particle formation may come about from crossing the fluid–solid boundary (F–S), or the system may first undergo a liquid–liquid (L–L) phase separation followed by solidification.
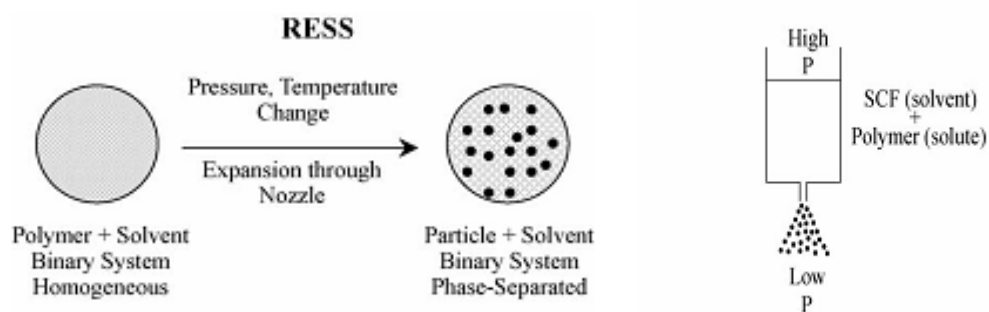
Figure 2.1 Schematic representations of the RESS process and its operational
(Sang-Do Yeo, 2005)
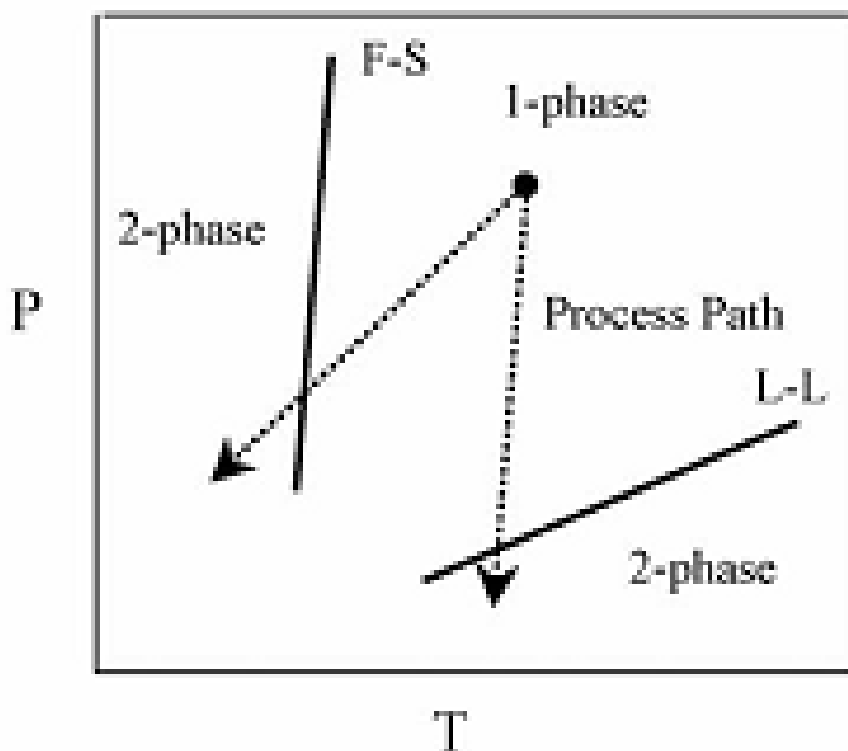
Figure 2.2 Process pathways in the P-T projection (Sang-Do Yeo, 2005)

2.2 Selection of supercritical fluids (SCF)

SCF is defined as a substance under supercriticals conditions, that is, above its critical pressure and temperature. **Figure 2.3** illustrates a pressure-temperature diagram of a substance indicating the supercritical region. The critical pressure (P_c) is the pressure which causes the gas to become a liquid at the critical temperature. Above the critical temperature (T_c), a liquid phase will not appear no matter how much the pressure is increased. The density of a substance at the critical point is call the critical density (ρ_c). The critical temperatures, pressures, and densities of some common solvents are listed in **Table 2.1.**
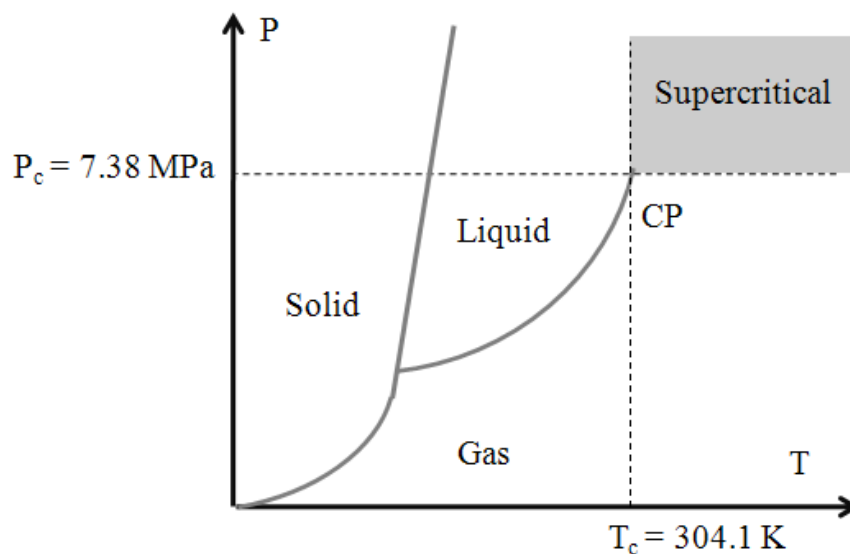
Figure 2.3 Phase diagram of substance approaching the supercritical phase

Table 2.1 Critical properties of selected solvents (McHugh and Krukonis, 1994)

Solvent	Critical Temperature (T_c; °C)	Critical Pressure (P_c; bar)	Critical Density (ρ_c; g/ml)
Ammonia	132.5	113.5	0.24
Benzene	129.0	48.9	0.30
n-Butane	152.0	38.0	0.23
Carbon dioxide	31.1	73.8	0.45
Chlorofluoromethane	28.9	39.5	0.58
Ethane	32.2	48.9	0.20
Ethanol	32.2	48.9	0.2
Ethylene	9.3	50.4	0.22
Isopropanol	235.3	47.6	0.27
Methanol	240.5	79.9	0.27
n-Propane	96.8	42.6	0.22
Propylene	91.9	46.2	0.23
Toluene	318.6	41.1	0.29
Water	374.2	221.2	0.34

A SCF exists in a homogeneous fluid phase possessing properties between those of gases and liquids, e.g. liquid-like solvent properties and gas-like viscosity, thermal conductivity and diffusivity. It is commonly accepted that the solvent power of SCF is mainly related to its density in the critical point region. A high density implies a power can be tuned by regulating its pressure or temperature. As demonstrated in **Figure 2.4**, a small change in the pressure or temperature of a SCF generally causes a large change in its density and thus its solvent power. This feature is beneficial for pharmaceutical solubilization, polymer plasticization, separation and extraction or organic solvents or impurities (Brunner, 2004). Even though the density of SCFs increases with pressure and becomes liquid-like, the viscosity and diffusivity remain between liquid-like and gas-like values. The gas-like properties of SCFs significantly enhance mass transfer that promotes selectivity for extraction and reactions. Additionally, SCFs have a very low surface tension, which allows efficient penetration into microporous materials. As a result, extraction of natural products can be expected to be more efficiently processed with SCFs than with conventional liquid solvents (Rantakyla, 2004). The combination of these unique properties makes SCFs excellent for use as solvents or reaction mediums. A comparison of properties of liquid, gas and SCF solvents is presented in **Table 2.2.**
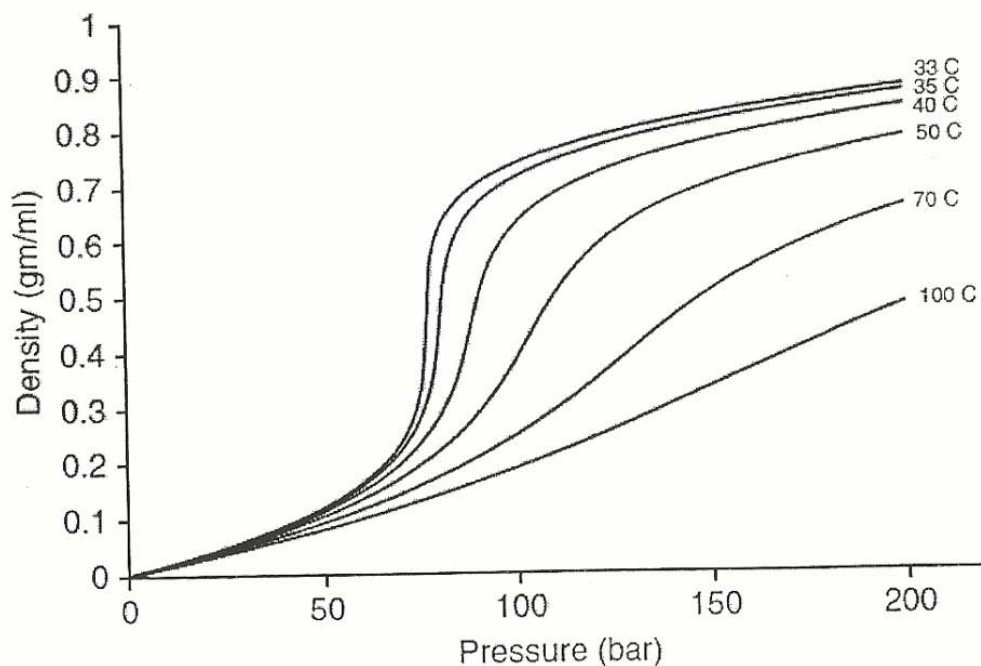
Figure 2.4 Variation of SCF density with pressure (Redrawn from Gupta and Shim (2007) and Brennecke and Eckert (1989))

Table 2.2 Selected properties of liquids, gases and supercritical fluids (Mchugh and Krukonis, 1994)

Properties	Liquid	Supercritical Fluid	Gas
Density (kg/m^3)	1,000	200 - 800	1
Viscosity (mPa.s)	0.5 – 1.0	0.05 – 0.1	0.01
Diffusivity (cm^2/s)	10^{-5}	$10^{-4} – 10^{-3}$	0.1

Various compounds can be used as SCF solvents. However, the most desirable SCF solvent for formation of encapsulation of foods and medicines is carbon dioxide (CO_2). With the ability to act both as electron donor and acceptor, CO_2 is a good solvent for non-polar and some polar compounds with low molecular weight, but a poor solvent for polar and most high molecular weight compounds (Hyatt, 1984).

CO_2 is also an inert, inexpensive, easily available, odorless, tasteless, environment-friendly, and GRAS (generally regarded as safe) solvent. Further, in SCF processing with CO_2, its near-ambient critical temperature makes it ideally suitable for thermolabile natural products.

For carbon dioxide, $P_c = 7.38$ MPa and $T_c = 304.1$ K, the state of the substance is called supercritical fluid (SCF) when both the temperature and pressure exceed the critical point values as schematically described in a pressure-temperature phase diagram which is shown in **Figure 2.3.**

Supercritical and liquid CO_2 can both be used as solvents. For liquid CO_2, the solvent power of SC-CO_2 is highly dependent on its temperature and pressure. At low pressure, the density of SC-CO_2 decreases dramatically with an increase in temperature, whereas changes in temperature have much less effect on the density at high pressure. Thus, to a first approximation, density, not pressure, is proportional to the solvent power of SC-CO_2. Based upon solubility measurement in range from ambient condition up to 1000 bar and 100°C, the solvent power of SC-CO_2 increases with density at given temperature, and increases with temperature at a given density (Smith et al., 1987; Ikusjima et al., 1991; Taylor, 1996). The density dependence of the solvent power can be observed through the relationship between the density and dipolarity/polarizability (π^*), a solvent-strength parameter of SC-CO_2 as shown in **Figure 2.5.**
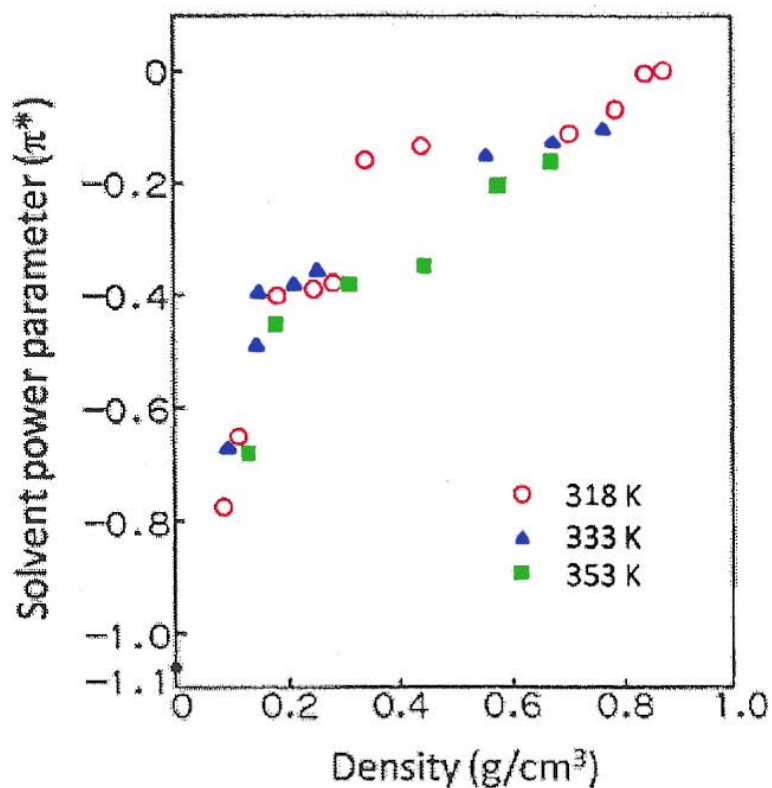
Figure 2.5 Effect of density on solvent power (π^*) of SC-CO_2 (Ikushima et al., 1991)

The environmentally benign nature of CO_2 is known as a result high bonding stability in its molecule. CO_2 has a symmetrical molecular structure without lone pair on the central atom. Thus, it is a good solvent for hydrocarbons and non-polar solids with low molecular weight, but a poor solvent for polar and most high molecular weight compounds (Hyatt, 1984). The solubility of a compound in SC-CO_2 strictly depends on the chemical groups available in the compound molecules, e.g. aromatic hydrocarbons, phenols, aromatic carboxylic acids, pyrones and lipids (Werling and Debenetti, 1999). As the number of carbon atoms increases and following the introduction of pair functional groups, the solubility decreases dramatically with pressure up to 40 MPa. This feature provides the possibilities for fractionating extraction of complex carbon compounds. An excellent summary on the solvent behavior of SC-CO_2 has been given by Stahl et al. (1980).

2.3 Expansion path

The expansion path can affect on the formation of the encapsulated particles as shown in **Figure 2.6.**
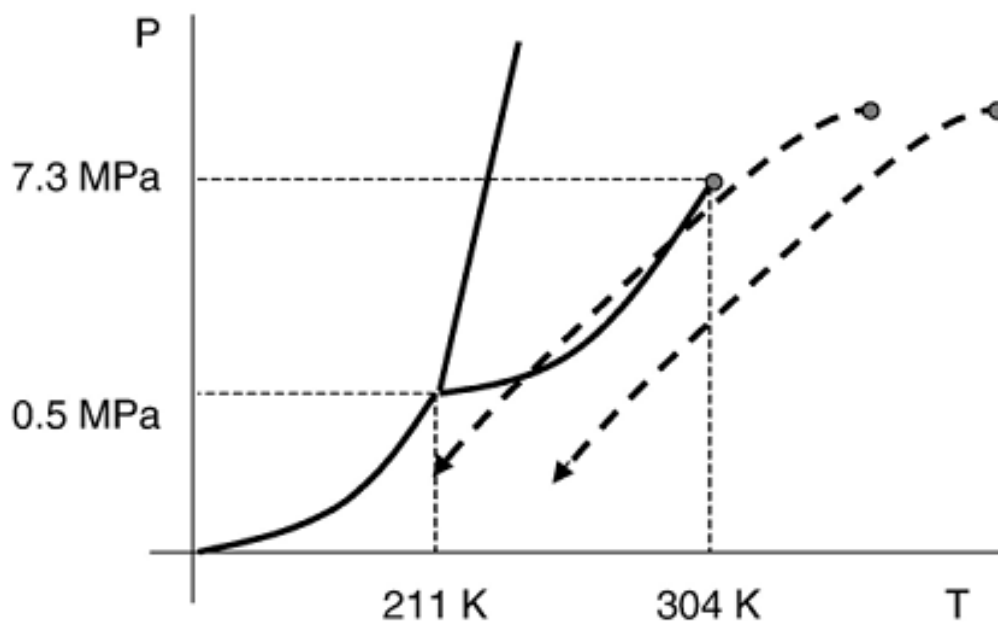
Figure 2.6 Depressurization of CO_2 on P-T diagram (Martin, 2008)

Depending on the pre-expansion pressure and temperature, the expansion trajectory may cross the vapor-liquid saturation line of CO_2, thus leading to the formation of liquid CO_2 droplets. It will affect morphology that make the bigger particles in this case, due to an early nucleation in the nozzle with strong particle growth by coagulation caused by high particle concentrations (Martin, 2008).

2.4 Selection of substance as active drug

Menthol is a terpenoid, found in the essential oils of the mint family (*Mentha spp*), such as peppermint, spearmint and others. A typical image of peppermint leaves as a source of menthol is shown in **Figure 2.7.**

Figure 2.7 Peppermint leaves (Menthol cigarettes no harzard to smoking, 2554)

Menthol ($C_{10}H_{20}O$) is solid at room temperature, forming long crystals that have a fatty touch. Several isomers of menthol exist. Some isomers will provide a menthol smell, others will not. Normally occurring menthol, with the strongest smell, is (-)-menthol as shown in **Figure 2.8.**
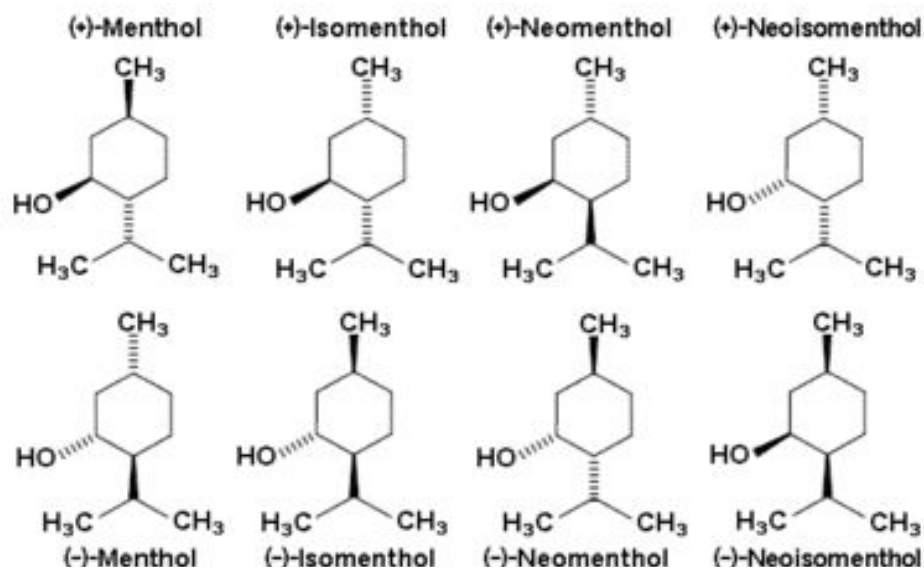
Figure 2.8 Structure of menthol and isomers (Food-Info, 2554)

Menthol is not or poorly soluble in water, but readily soluble in alcohol or oils. Besides the use as an aroma in many different food products (especially dental products, such as chewing gum, cough drops and confectionary, such as mints), menthol is contained in non-prescription products for short-term relief of minor sore throat and minor mouth or throat irritation, for example in lip balms and cough medicines. It is classed as an antipruritic, which reduces itching. Menthol is also contained in combination products used for relief of muscle aches, sprains, and similar conditions, as well as in decongestants. In addition, it is used as an additive in certain cigarette brands, both for flavor and to reduce the throat and sinus irritation caused by smoking. Menthol also is a common ingredient in mouthwash.

2.5 Selection of substance as coating material

The selection of a coating material is one of the most widely investigated topics for many studies. Criterion of this issue depends on the surface properties of the desired particle. Recently, many biodegradable polymers, such as PEG, PLGA and etc., have been used in pharmaceuticals and cosmetics as coating materials. Polymers are typically used by dissolution in supercritical carbon dioxide (SC-CO$_2$) because of strong interactions with CO$_2$. Moreover, this method is fully approved as relatively non-toxic by the U.S. Food and Drug Administration (FDA). Additionally, solubility of polymers in SC-CO$_2$ can be increased by pressure increase or adding a minimal amount of co-solvent.

PEG is one of the commonly used compounds in the pharmaceutical industry because of its hydrophilic nature. It can be produced by polymerization of ethylene oxide which is commercially available over a wide range of molecular weights from 300 g/mol to 10 ,000,000 g/mol and used with the other types of polymers for modification of polymer matrix properties. PEG is available in different states such as liquid or solid depending on the molecular weight. In the solid state, PEG is mainly used in particle form for pharmaceutical applications, such as drug carriers. In this application, the particle shape, size, density and particle size distribution are very important. Since the melting point (T$_m$) of PEG is not high (around 335 K), milling or grinding is not easy as demonstrated by its chemical structure in **Figure 2.9.**
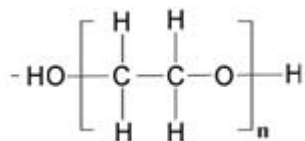
Figure 2.9 Chemical structure of PEG

2.6 Encapsulated particles

Encapsulated particles are produced for many applications such as controlling the release of active material in a desired quantity and location, increasing the dissolution rate of slightly water-soluble materials and modifying the surface properties of particles used in pharmaceuticals, catalysts, cosmetics, the printing industry and energetic materials. Encapsulated particle or composite particles are defined as either the dispersion of one (or more) solid phase(s) in another continuous solid phase, called a matrix structure, or a core of a material coated by another solid phase, called a reservoir structure. Matrix and reservoir structures have been termed by some researchers as "microsphere and microencapsule", as shown in **Figure 2.10.**

(A)   (B)
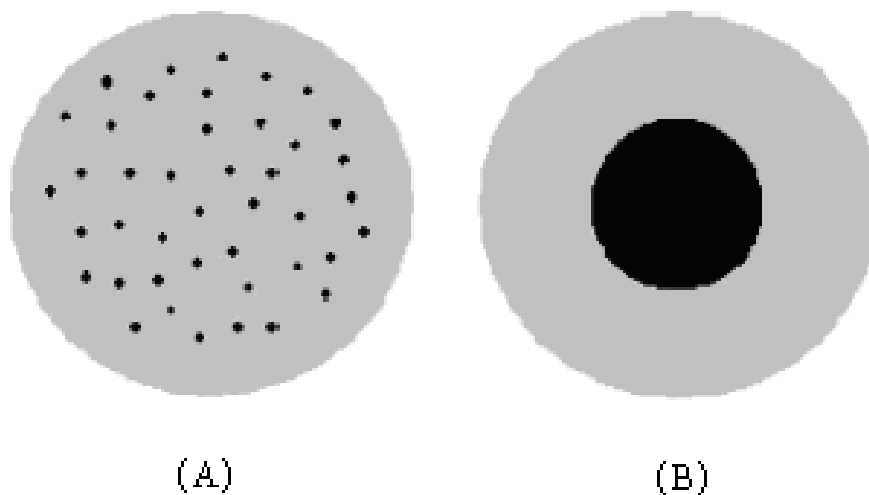
Figure 2.10 (A) Matrix structure, microsphere, and (B) a reservoir structure, microencapsule (Bahrami and Ranbarian, 2006)

The morphology of the resulting solid material both depends on the material structure (crystalline or amorphous, composite or pure substrate) and of the RESS parameters (temperature, pressure drop, distance of impact of the jet against the surface, dimensions of the atomization vessel, nozzle geometry).

2.7 Joule–Thomson effect

While spraying the saturated solution through the nozzle, when a non-ideal gas suddenly expands from a high pressure to a low pressure, there is often a temperature change. This phenomenon, the "Joule–Thomson effect" appears at the end of nozzle. Officially, the ratio of $\frac{\Delta T}{\Delta P}$ is known as the Joule-Thomson coefficient. It is a diabatic effect, in which the pressure change occurs too quickly for significant heat transfer. For many gases at room temperature, the $\frac{\Delta T}{\Delta P}$ ratio is positive. Thus, a pressure drop is accompanied by a temperature drop. For example, if a tank of CO_2 is opened to the atmosphere, one can see a spray of fine dry ice particles emerging at about –78°C. The phenomenon results in the deformation of the encapsulated particles because PEG is soluble in water. A more in-depth description of the Joule-Thomson coefficient is given by the **Equation 2.1**, which is discussed fully in the derivations manual discussion of this effect.

$$\mu_{JT} \equiv \left(\frac{\partial T}{\partial P}\right)_H = \frac{V}{C_P}(\alpha T - 1) \tag{2.1}$$

From Huang et al., 2005, temperature at nozzle was kept around 80-100°C. They reported the chemical potential; $\quad \mu_{CO_2} = 1.084 \pm 0.050 \cdot 10^{-5}\, \frac{K}{Pa}$

To control isothermal expansion, the instrument was installed heating zone at the nozzle for preventing the Joule-Thomson effect. The temperature at the nozzle was around 40°C (313 K).

2.8 Fluid mechanics along the nozzle

Many studies have been conducted on fluid mechanics along nozzles. They separates three regions as shown in **Figure 2.11** consisting of inlet the region of the nozzle, the nozzle itself (capillary) and the expansion region (supersonic free jet). However, when the fluid impact mach disc (plate) pressure increases up to the ambient pressure, accompanied by an increase in temperature, the sudden increase in pressure and temperature causes the evaporation of CO_2 droplets, if they were formed.
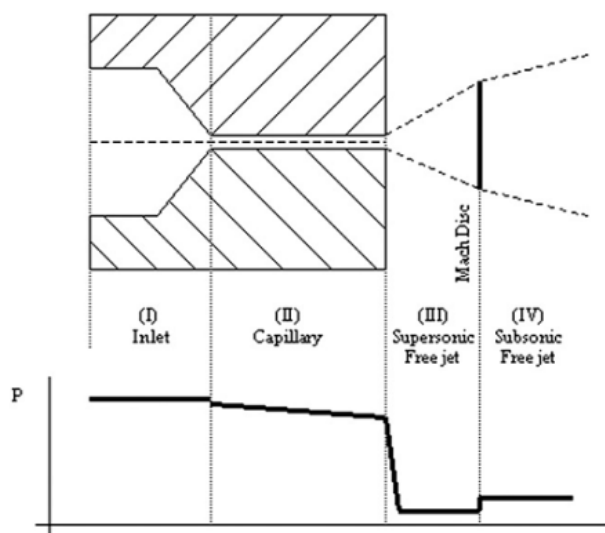
Figure 2.11 Schematic diagram of a RESS expansion device with approximate pressure profile (Martin, 2008)

The Match Disc or Plate (Sampling position for scanning electron microscope/ Optical microscope) should be considered. The Plate should be installed in supersonic free jet. Moreover, the distance between plate and the edge of nozzle should be also considered in order to get undamaged particles. This study found that the best position for the plate is 45 cm from the edge of nozzle.

2.9 Degree of supersaturation

For the characterization of particle formation in RESS process, Debenetti et al., 1990 and Türk et al., 2000 adapted the classical theory of homogeneous nucleation taking into account the highly non ideal behavior of supercritical fluids. This is done by modifying the definition of the supersaturation by the inclusion of a thermodynamic correction factor

The degree of supersaturation (*S*) of real fluid is calculated using **Equation (2.2)** expressed in M. Türk, 2000.

$$S = \frac{y_{solute}\ \emptyset(T,P,y)}{y_{eq}\,\emptyset(T_{eq},P_{eq},y_{eq})} \tag{2.2}$$

For obtaining $\emptyset$, investigation of PVT is necessary. However,

For ideal solution $\emptyset(T_{eq}, P_{qe}, y_{eq}) = \emptyset(T, P, y)$ so the expression is $S = \frac{y_{solute}\ (T,P)}{y_{eq}\ (P_{eq},T_{eq})}$

Both particle formation and nucleation growth are faster at high degree of supersaturation. Generally, a larger number of smaller particles are produced when the degree of supersaturation is increased.

Figure 2.12 illustrates the relation of the state of the system and the degree of supersaturation. While the degree of supersaturation is less than one, the system is in the single phase. During spraying the solution through the nozzle, the degree of saturation will change to have a value greater than 1. At the degree of supersaturation equals 1, the solution start to precipitate into solid particles. When the degree of supersaturation is greater than one, the system becomes two phases.
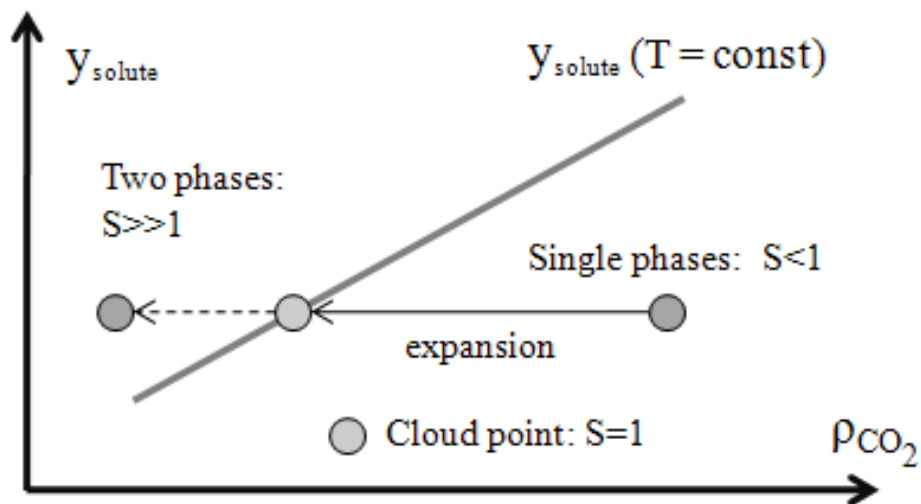
Figure 2.12 Schematic solubility vs density diagram for a mixture composed of a solute and a SCF (Martin, 2008)
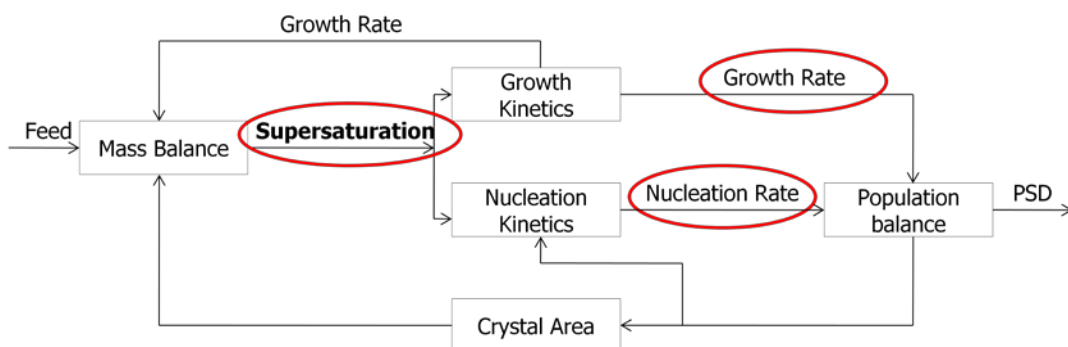
Figure 2.13 Information diagram showing feed back interaction of crystallization factors

Figure 2.13 shows that the degree of supersaturation at the edge of nozzle relates with growth rate and nucleation rate of the obtained particles. Case I, there is low solubility of solute in the autoclave. During spraying, the solvent will diffuse out the solution led to be high degree of supersaturation at the edge of nozzle resulting to occur

fast nucleation rate and low opportunity to occur surface integration. These reasons cause to get small particle size and large number of particles that is shown in **Figure 2.14.**
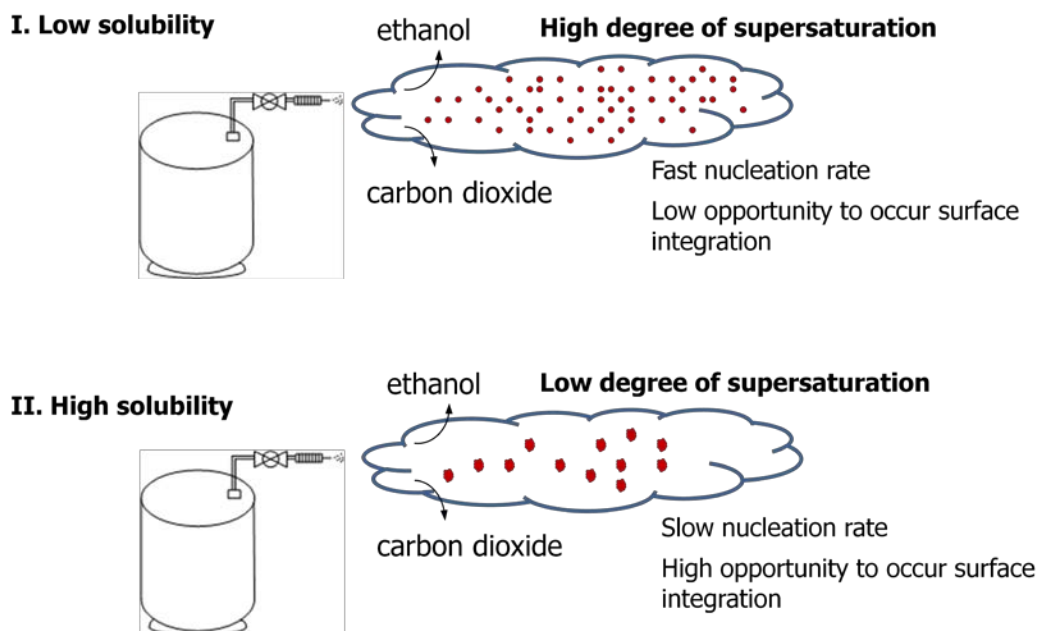
Figure 2.14 Modeling explaining the relationship of solubility of solute and degree of supersaturation.

Moreover, nucleation rate and particle growth rate also affect on the morphology and size of particle. Two mechanisms have to be considered: coagulation, which is the growth by collision of particles. Micrometer-sized or smaller particles can stick strongly to any surface they contact. As a consequence of this phenomenon along with Brownian motion, aerosol particles collide and stick together due to a process called thermal coagulation. The result is that at high concentration conditions, the average particle size of aerosol increases and number concentration decreases with time.

The other mechanism is condensation, which is the deposition of the molecules on the surface of the particles. These two mechanisms can occur after nucleation of particle that are shown as in **Figure 2.15**.
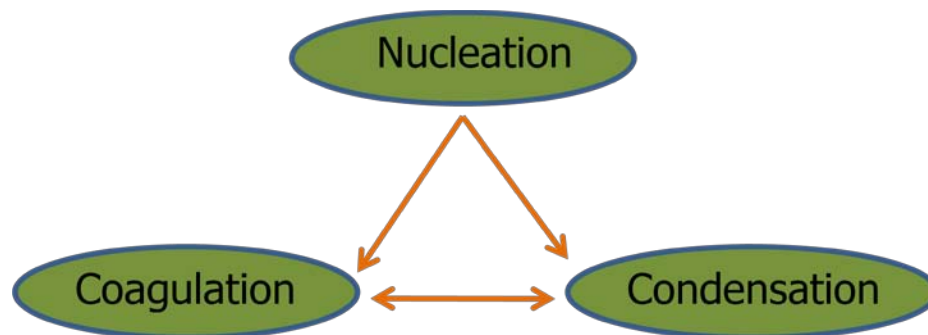
Figure 2.15 Mechanism of precipitation and particle growth (M. Türk, 2009)

2.10 Modeling of solubility in SCF solvent with equation of state

In SCF precipitation processes for particle production, nucleation is very strong function of supersaturation, which depends on solubility. Solubility also can have a noticeable effect on precipitation kinetics which, in turn yields the size and morphology of the precipitated product (Shekunov, 1999). Depending on the aim of the process, either a high solubility or low solubility may be requires. High solubility in SC-CO_2 is required in a process based on the rapid expansion of supercritical solution (RESS) technique (Thakur and Gupta 2005). On the other hand, the anti-solvent process, such as gas anti-solvent (GAS), supercritical anti-solvent (SAS) and solution enhanced dispersion by supercritical fluid (SEDS), require low solubility in a mixture of CO_2 and organic solvent (Chattopadhyay and Gupta, 2001). Thus the knowledge of solubility of the target material in SC-CO_2 is essential both for the initial feasibility study and final process design of a successful process.

Estimation of the equilibrium solubilities using a thermodynamic model is a reliable alternative way for obtaining the solubility data of the solutes in SCFs. The most common thermodynamic models are cubic equations of state (EOS). The most used models are those from van der Waals series e.g. Peng-Robinson (PR), Soave-Redlich-Kwong (SRK) and Sanchez-Lacombe lattice fluid model. Several mixing and combining rules, like classical van der Waals mixing rules, are utilized to incorporate a solution

model into EOS. Together with several solute properties, all of these models require at least one parameter exhibiting interactions between components in the solution, which in most cases, must be determined from existing experimental solubility data.

In many cases, for most pharmaceutical materials, the necessary solute properties (e.g. critical properties, molar volume, sublimation pressure) are not yet available in the literature and need a prior experimental determination or prediction by several estimations. Therefore, apart from selecting the appropriate EOS and mixing rules, extreme caution should be made in applying these additional estimations.

The general method for estimation of solubility of solid species (solute, 2) in the SCF phase starts with satisfying the phase equilibrium condition of equal component fugacities in the solid and SCF phases follow **Equation 2.3**:

$$f_2^{solid} = f_2^{SCF} \tag{2.3}$$

For the SCF phase, the solute mole fraction (y_2) can be written as a function of fugacity (f_2^{SCF}) and fugacity coefficient (φ_2^{SCF}) shown in **Equation 2.4**:

$$y = \frac{f_2^{solid}}{\varphi_2^{SCF} P} \tag{2.4}$$

Where P is the total pressure. Assuming that the SCF is not absorbed by the solid solute, the solid phase may be considered as a pure phase, and the fugacity in the solid phase (f_2^{solid}) can be written as **Equation 2.5**:

$$f_2^{solid} = P_2^{Solid} \phi_2^{SCF} exp \left(\int_{P_2^{Solid}}^{P} \frac{v_2^{Solid}}{RT} dP \right) \tag{2.5}$$

Where T is temperature, v_2^{Solid} is the molar volume of the solid solute (m^3/mol), P_2^{Solid} is vapor pressure or sublimation pressure of the solid solute, and R is gas constant (8.314 J/mol·K). For most solutes which do not possess a strong tendency of association, the

values of ϕ_2^{SCF} can be taken to 1 due to the low vapor pressures. In addition, due to the fact that solids are incompressible, it is reasonable to assume that the values of v_2^{Solid} are independent of pressure. Hence, the solubility of a solid solute *(y₂)* in a SCF can be written as **Equation 2.6**:

$$y_2 = \frac{P_2^{Solid}}{P} \left[\frac{1}{\phi_2^{SCF}} \, exp \left(\frac{v_2^{Solid} \, (P - P_2^{solid})}{RT} \right) \right] \qquad (2.6)$$

Where the term $\left[\frac{1}{\phi_2^{SCF}} \, exp \left(\frac{v_2^{Solid} \, (P - P_2^{solid})}{RT} \right) \right]$ is called the enhancement factor and $\frac{P_2^{solid}}{P}$ is the solute in the ideal gas. The fugacity coefficient of the solid solute in SCF phase (φ_2^{SCF}) can be calculated from (Prausnitz, 1986) shown in **Equation 2.7**:

$$RT\varphi_2^{SCF} = \int_v^\infty \left[\left(\frac{\partial P}{\partial n_2} \right)_{T,v,n_1} - \frac{RT}{v} \right] dv - RTln \left(\frac{Pv}{RT} \right) \qquad (2.7)$$

Where n_2 is the number of moles of solid solute, n_1 is the number of moles of CO_2, and *v* is the molar volume of the mixture. An appropriate equation of state is used to evaluate the integration and the value of *v*.

SCF precipitation processes are used to micronized a number of pharmaceutical materials, which involve various types of molecules, from simple to very complex. To select a reliable and appropriate model of EOS and mixing rules that contains all the molecular, the relevant models were examined. Most of the van der Waals family models (PR,SRK and PT) are well correlated with solubility data of simple sphere-like molecules, On the other hand, the Sanchez-Lacombe model has been developed on the basis of the lattice fluid model for treating chain-like molecules (Colussi, 2006). It should be remarked that these two models are mean-field models, which means that they cannot be applied in the vicinity of the critical point with good results.

In this study, menthol and commercial biodegradable polymer poly(ethylene)glycol with molecular weight equal to 6000 (PEG6000) and SC-CO_2 with

ethanol as co-solvent are mixed to provide SCF solutions for the RESS process. Data about the solubility of menthol and PEG6000 in a SCF solvent does not appear to be available in the current literature. Therefore the solubility of menthol and the solubility of PEG6000 in the SCF solvent have been adapted to predict their solubility in SC-CO_2.

Taking into consideration that the majority of PEG molecules are long-chain, not sphere-like, it is therefore reasonable to use Sanchez-Lacombe EOS to evaluate the PEG6000 solubilities in the SCF solvent. Together with a thermodynamically consistent expression of fugacity coefficients, proper estimations of the EOS characteristic parameters are made in order to obtain a reliable evaluation of the PEG6000 solubilities. The Sanchez-Lacombe EOS has been used successfully for modeling solute in many polymer/SC-CO_2 systems (Sarah 2003 et al., Mishima 2006 et al., Li, 2007 et al.).

2.2.1 Solubility of PEG6000 in SC-CO_2; Sanchez-Lacombe EOS (Sanchez and Lacombe, 1976)

According to the lattice theory of Sanchez-Lacombe, a pure fluid can be viewed as a mixture of segments and holes which occupy the sites of lattice, the lattice-fluid model of EOS for a pure component has the following form:

$$\tilde{P} + \tilde{\rho}^2 + T\left[ln(1-p) + \left(1 - \frac{1}{r}\right)\tilde{\rho}\right] = 0 \qquad (2.8)$$

Where

$$\tilde{P} = \frac{P}{P^*} \qquad (2.9)$$

$$\tilde{T} = \frac{T}{T^*} \qquad (2.10)$$

$$\tilde{\rho} = \frac{\rho}{\rho^*} \qquad (2.11)$$

$$\rho^* = \frac{M_w}{v^*} \tag{2.12}$$

$$r = \frac{P^* v^*}{RT^*} \tag{2.13}$$

Where $\tilde{P}$, $\tilde{T}$ and $\tilde{\rho}$ are the reduced parameters, P^*, T^*, ρ^* and v^* are the characteristic pressure, temperature, density and molar volume, respectively. M_w is the molecular weight, R is the gas constant $(8.31451\,\mathrm{J \cdot mol^{-1} \cdot K^{-1}})$ and r is the size parameter, which represents the number of lattice sites occupied by molecule.

In order to extend the use of this model to mixtures, the mixing rules described below are applied (Xiong and Kiran, 1994).

$$\frac{1}{v^*} = \sum_i \frac{\phi_i}{v_i^*} \tag{2.14}$$

$$\phi_i = \frac{\frac{W_i}{\rho_i^*}}{\sum_j \frac{W_j}{\rho_j}} \tag{2.15}$$

$$\frac{1}{M_w} = \sum_i \frac{\phi_i}{M_{w,i}} \tag{2.16}$$

Where ϕ_i, W_i and $M_{w,i}$ are respectively the close packed volume fraction, mass fraction and molecular volume weight of the component i. The characteristic pressure for the mixture (P^*) is given by the following equations:

$$P^* = \sum_j \phi_j P_j^* - RT \sum_j \sum_{i<j} \phi_i \phi_j \chi_{ij} \tag{2.17}$$

$$\chi_{ij} = \frac{P_i^* + P_j^* - 2(1-k_{ij})\sqrt{P_i^* P_j^*}}{RT} \tag{2.18}$$

Where k_{ij} is the binary interaction parameter. The characteristic temperature for the mixture (T^*) is given by the following equations:

$$\tilde{T} = \frac{P^* v_0}{R} \tag{2.19}$$

$$\frac{1}{v_0} = \sum_i \phi_i \left(\frac{P_i^*}{RT_i^*} \right) \tag{2.20}$$

The Sanchez-Lacombe EOS together with mixing rules, **Equation (2.8) – Equation (2.20)**, were used to model the phase behavior of the system CO_2 + PEG6000 + ethanol at the upstream condition of the RESS process. For the scope of this study, RESS experiments were performed under certain pressure and temperature conditions. Modeling the solubility of a solid in the SCF solvent with Sanchez-Lacombe EOS requires several characteristic parameters of pure components. Binary interaction parameters are necessary to represent the behavior of the multi-component system. For the CO_2 (1) + PEG6000 (2) + ethanol (3) ternary system, the value of the pure component parameters were taken from the literature as the basic input. These values are presented in **Table 2.3** and **Table 2.4.**

The binary interaction parameters are independent of pressure, but a function of temperature. Weidner et al., (1997) have studied phase equilibrium of SC-CO_2 + PEG4000 systems. They reported the useful correlations between the binary interaction parameter and temperature for Sanchez-Lacombe EOS. The dependence of binary interaction parameter (k_{12}) on temperature $(T(K))$ in the range of 313.4-344.75 K can be expressed by:

$$k_{12} = -6.43 \times 10^{-6} T(K) + 1.45 \times 10^{-2} \tag{2.21}$$

Furthermore, the interaction parameter between CO_2 and ethanol system (Joung, 2001) can be expressed by:

$$k_{13} = 2.41 \times 10^{-4}T(K) - 4.84 \times 10^{-2} \tag{2.22}$$

The interaction parameter k_{13} has a positive inclination with temperature, while k_{12} has a slight negative inclination with temperature. The inclination tendency of k_{13} is significantly higher than that of k_{12}. Thus the influence of the polar end groups is stronger than that of PEG because it generally becomes stronger with decreasing molecular weight (Wiesmet, 2000).

Matsuyama et al., (2006) reported that binary interaction parameter between PEG and ethanol (k_{23}) equals -0.042 from their experimental results. The value of k_{23} is very large as compared to other values. This is caused by the intermolecular interaction between the polar end groups of PEG and ethanol.

Table 2.3 Molecular weights (M_w) and structures of pure components.

Component	M_w (g mol^{-1})	Molecular structure
CO_2 (1)	44.01	O=C=O
PEG (2)	8800	$-HO{\left[\!\begin{array}{c} H\ \ H \\ -C-C-O- \\ H\ \ H \end{array}\!\right]}_n\!H$
Ethanol (3)	46.07	$H-\overset{\overset{\displaystyle H}{\mid}}{C}-\overset{\overset{\displaystyle H}{\mid}}{C}-O-H$

[a] average value

Table 2.4 Characteristic parameters of pure components for Sanchez-Lacombe EOS.

Component	$P^*(MPa)$	$T^*(K)$	$\rho^*(kg/m^3)$	Reference
CO_2 (1)	574.5	305.0	1510	Xiong 1994, Kiszka 1998
PEG (2)	492.2	656.0	1177.6	Rodgers 1993
Ethanol (3)	1069.0	413.0	963.0	Sanchez and Lacombe, 1976

Table 2.5 Selected interaction parameters for CO_2 (1) + PEG6000 (2) + Ethanol (3) system at 313 K.

k_{12}	k_{13}	k_{23}
0.012487	-0.048159	-0.4200

$$CO_2 - PEG6000 < CO_2 - Ethanol < PEG6000 - Ethanol$$

The chemical structure plays an important role in the interactions between CO_2 – PEG6000, CO_2 – Ethanol, PEG6000 – Ethanol. Because of the symmetry of the molecular structure, CO_2 has no dipole moment and a very low polarity. The van der Waals forces in CO_2 are generally responsible for their interactions with other molecules. Since ethanol is polar and capable of being both donor and acceptor of hydrogen bonds, it has a fairly high polarity and forms self-association through hydrogen bonding with CO_2 molecules. Furthermore, at the pressure and temperature conditions in this study, CO_2 and ethanol form a completely miscible phase, according to vapor-liquid equilibrium data in (Suzuki and Sue, 1990; Jenning et al., 1991;Yoon et al., 1993). In case of CO_2 – PEG6000 binary mixtures, the polarity and van der Waals forces of CO_2 are too weak for

PEG6000. For PEG6000 – ethanol binary mixtures, ethanol has matched polarity and forms self-association with PEG6000. The bonding occurs at their polar end groups. However, the polarity matching to PEG6000 and the degree of ethanol self-association with PEG6000 is reduced in the ternary mixtures. On the other hand, it may be considered that PEG6000 and ethanol form microemulsion in the SC-CO_2 single phase. In this case, ethanol is considered as a co-solvent. Consequently, it is reasonable to conclude that CO_2 + PEG6000 + ethanol mixture forms a single-phase supercritical solution in the experimental conditions of this study.

The interaction parameters χ_{ij} corresponding to the calculated values of k_{ij} were determined by using **Equation (2.18)** with numerical values presented in **Table 2.4** and **Table 2.5**:

$$\chi_{12} = 6324.9197 \, \text{mol} \cdot \text{m}^{-3}$$
$$\chi_{13} = 259.7652 \, \text{mol} \cdot \text{m}^{-3}$$
$$\chi_{23} = -191685.8052 \, \text{mol} \cdot \text{m}^{-3}$$

Let W_1, W_2, W_3 be the equilibrium phase composition (on the basis of mass fraction) of the ternary mixture, governed by the equal constrains of the sum of the mass fraction equal to unity:

$$W_1 + W_2 + W_3 = 1 \tag{2.23}$$

The closed pack volume fractions of the components can be expressed as functions of the mass fractions by expanding **Equation (2.16).**

$$\phi_1 = \frac{\frac{W_1}{\rho_1^*}}{\frac{W_1}{\rho_1^*} + \frac{W_2}{\rho_2^*} + \frac{W_3}{\rho_3^*}} \tag{2.24}$$

$$\phi_2 = \frac{\frac{W_2}{\rho_2^*}}{\frac{W_1}{\rho_1^*}+\frac{W_2}{\rho_2^*}+\frac{W_3}{\rho_3^*}} \tag{2.25}$$

$$\phi_3 = \frac{\frac{W_3}{\rho_3^*}}{\frac{W_1}{\rho_1^*}+\frac{W_2}{\rho_2^*}+\frac{W_3}{\rho_3^*}} \tag{2.26}$$

The corresponding expressions for the characteristic parameters of the mixture were derived **Equation (2.12)** – **Equation (2.26)** by use of some pre-determined numerical values. A series of steps was taken in the following order:

I. The characteristic pressure P^* was obtained by substitutions of **Equation (2.24)** – **Equation (2.26)** and the values of R, T, P_1^*, P_2^*, P_3^*, χ_{12}^*, χ_{13}^* and χ_{23}^* into the expanded form of **Equation (2.18).** The result is followed **Equation 2.27.**

$$P^* = \phi_1 P_1^* + \phi_2 P_2^* + \phi_3 P_3^* - RT[\phi_1\phi_2\chi_{12} + \phi_1\phi_3\chi_{13} + \phi_2\phi_3\chi_{23}] \tag{2.27}$$

II. To determine the characteristic temperature T^*, an expression for v_0 was first obtained by using the expanded form of **Equation (2.20).** The result is followed **Equation 2.28.**

$$\frac{1}{v_0} = \frac{\phi_1 P_1^*}{RT_1^*} + \frac{\phi_2 P_2^*}{RT_2^*} + \frac{\phi_3 P_3^*}{RT_3^*} \tag{2.28}$$

and followed by substitutions into **Equation (2.26).**

III. The characteristic volume v^* was determined by the expansion of **Equation (2.14).).** The result is followed **Equation 2.29.**

$$\frac{1}{v^*} = \frac{\phi_1}{v_1^*} + \frac{\phi_2}{v_2^*} + \frac{\phi_3}{v_3^*} \tag{2.29}$$

where v_1^*, v_2^* and v_3^* were first determined using **Equation (2.12).**

IV.   The size parameter r was determined by substitutions into **Equation (2.11)**

V.   The effective molecular weight of the mixture M_w was determined by substitions of **Equation (2.24)** – **Equation (2.26)** and the numerical values of molecular weights into the expanded form of **Equation (2.13)**. The result is followed **Equation 2.30:**

$$\frac{1}{M_w} = \frac{\phi_1}{M_{w,1}} + \frac{\phi_2}{M_{w,2}} + \frac{\phi_3}{M_{w,3}} \tag{2.30}$$

VI   The characteristic density ρ^* was obtained by **Equation (2.12).**

Selecting P = 15 MPa and T =313 K in **Equation (2.9)** and **Equation (2.10)**, the reduced pressure ($\widetilde{P}$) and temperature ($\widetilde{T}$) were obtained, respectively. The Sanchez-Lacombe EOS in **Equation (2.8)** and the equality constraint in **Equation (2.23)** were used to perform the ternary phase equilibrium calculations. A system of two equations and four variables were formed and can be expressed by system of **Equation 2.31:**

$$F(W_1, W_2, W_3)\widetilde{P} + \tilde{\rho}^2 + T\left[\ln(1-p) + \left(1 - \frac{1}{r}\right)\tilde{\rho}\right] = 0$$
$$G(W_1, W_2, W_3) = W_1 + W_2 + W_3 - 1 = 0 \tag{2.31}$$

The results were shown in **Table 3.1** and **Figure 3.3, Chapter III**.

2.2.2 Solubility of menthol in SC-CO₂; SRK EOS (Soave-Reddlich-Kwong)

Knowledge of menthol solubility in supercritical CO_2 is crucial in the investigation of the RESS of menthol using CO_2 as the processing solvent. The limitation of the menthol amount dissolvable in CO_2 at specified pre-expansion temperature and pressure was estimated using a mathematical thermodynamic model. Due to the accuracy of menthol solubility prediction with experimental data, this study selected the SRK cubic equation of state (EOS) together with the one fluid van der Waals mixing rule were used to model the phase behavior of the system CO_2 + menthol at the upstream condition of the RESS process. For the scope of this study, RESS experiments were performed under certain pressure and temperature conditions. Determining of the solubility of menthol in SC-CO_2 with the SRK equation of state requires several values of pure components as shown in **Table 2.6** (Sovová, 2007).

The modified thermodynamic model (SRK) is expressed in **Equation 2.32.**

$$P = \frac{RT}{v - b_{mix}} - \frac{a_{mix}}{v(v + b_{mix})} \tag{2.32}$$

The one fluid van der Waals mixing rule are showed in **Equation (2.33)** and **Equation (2.34)**:

$$a_{mix} = \sum_i \sum_j x_i x_j a_{ij} \tag{2.33}$$

$$b_{mix} = \sum_i \sum_j x_i x_j b_{ij} \tag{2.34}$$

where a_{mix} and b_{mix} are the mixture energy and co-volume parameter, respectively. The geometric mean rule is applied to determine the cross-energy parameter a_{ij} and co-volume parameter by following **Equation (2.35)** and **Equation (2.36).**

$$a_{ij} = (a_{ii} a_{jj})^{0.5} (1 - k_{ij}) \tag{2.35}$$

$$b_{mix} = \sum_{i=1}^{N_C} x_i b_{ii} \tag{2.36}$$

Table 2.6 Carbon dioxide and menthol properties used in calculation (Sovová, 2007).

Property	CO_2	Menthol
Molar mass $(g \cdot mol^{-1})$	44.01[a]	156.27
Melting temperature (K)	-	297.3[b]
ΔH fusion $(J \cdot mol^{-1})$	-	12189.07[b]
T_C(K)	304.1[a]	384.85[c]
P_C(MPa)	7.3765[a]	2.7104[c]
V^S $(cm^3 \cdot mol^{-1})$	-	156[d]

[a] Stateva and Tsvetkov (1991); [b] Perry 's Chemical Engineers' Handbook

[c] Rowley et al., 2006; [d] Estimated value

Solving the equation of state (SRK) by following **Equation (2.31) - Equation (2.36)**. The results of the solubility calculations were shown in **Table 3.2** and **Figure 3.14, Chapter III**.

CHAPTER III

EXPERIMENTAL

3.1 RESS apparatus

In accordance with the objectives of this study, formulating encapsulated particles through the rapid expansion of supercritical carbon dioxide process (RESS) with ethanol as co-solvent was studied in detail. A series of batch RESS experiments were carried out by using the apparatus setup shown in **Figure 3.1** with and the actual instrument shown in **Figure 3.2**. Menthol/PEG6000 and ethanol were loaded into the autoclave and then the temperature of autoclave was increased until reaching the target temperature. Then CO_2 was supplied until the designated pressure was achieved by high pressure pump (PU-1580-CO_2; JASCO, Japan). The autoclave chamber was kept quiescent for 2 hours prior to spraying of the supercritical solution through a nozzle with an inner diameter of 0.3 mm. The spraying nozzle was covered with a heating coil to maintain the isothermal expansion condition at around 313 K. The obtained products were collected in a collecting chamber (I.D = 6 cm.) equipped with a HEPA filter to ensure the complete collection of the micronized product.
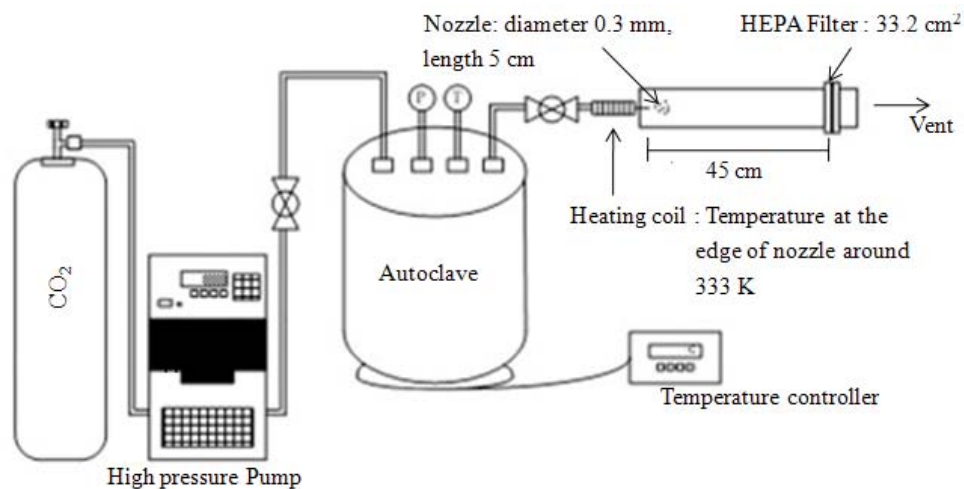
Figure 3.1 Schematic diagram of RESS apparatus
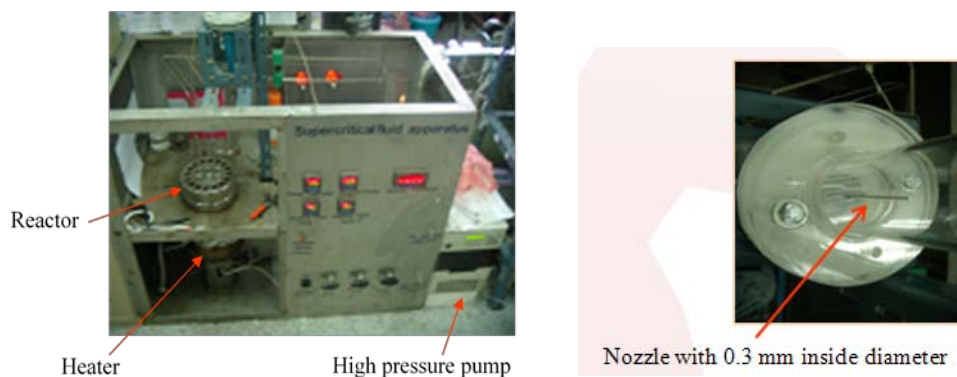
Figure 3.2 Actual RESS apparatus

The experiment was separated into 3 parts including micronization of menthol, micronization of PEG6000 and the formation of encapsulated particle of menthol and PEG6000. The RESS parameters which affected the formation of each part were carefully investigated.

3.2 Experimental condition

For the RESS process, the solubility of solute was necessary because the solution at supercritical state should be complete dissolution in order to maximize obtained product of each experiment. The solubility of solute at equilibrium could calculate from the equation of state that was shown in Chapter II.

3.2.1 Estimation of menthol solubility in carbon dioxide

The calculation of menthol solubility provided by Soave-Redlich-Kwong equation of state was shown in **Table 3.1** and **Figure 3.3.**

Table 3.1 Calculated mole fraction of CO_2 + menthol system

Temperature (K)	Pressure (MPa)	mole fraction of menthol
303 K	10	4.66E-02
	15	8.84E-02
	20	1.18E-01
313 K	10	2.53E-02
	15	1.08E-01
	20	2.29E-01
323 K	10	5.41E-03
	15	6.66E-02
	20	1.97E-01
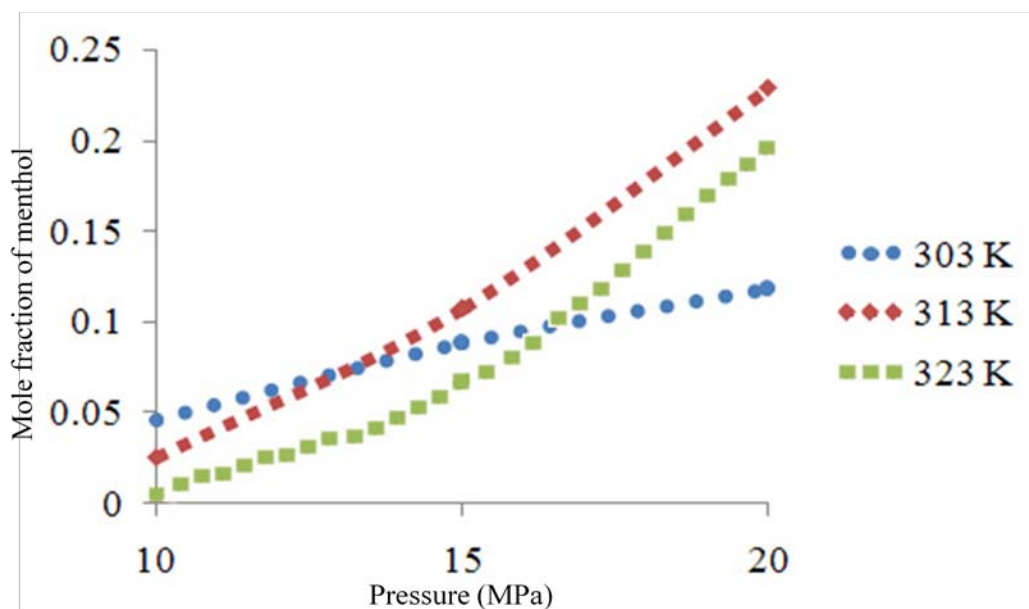
Figure 3.3 Estimation of solubility of menthol provided by Soave-Redlich-Kwong equation of state

The amount of menthol that was put in the autoclave should be less than amount of menthol at equilibrium state provided by Soave-Redlich-Kwong equation of state. Then the phase composition of experiment was considered that was shown in **Table 3.2**

Table 3.2 Example of experimental condition of micronized menthol at 313 K, 10 MPa, 10 wt% of ethanol

Substance	density (g/ml)	Flow rate (ml/min)	P (MPa) = 10	T (K) = 303	weight fraction	mol fraction	
			time (min)	mass (g)			solubility of menthol @ 313 K,10MPa (mole fraction),
CO_2	0.62	10	67	415.4	8.90E-01	9.00E-01	
Ethanol		volume (ml)					
	60	0.789		47.37	1.01E-01	0.98E-02	
Menthol				4	8.60E-03	2.40E-03	2.53E-02
PEG6000				0	0.00E+00	0.00E+00	

From **Table 3.2**, all of menthol was dissolved into supercritical state observed by the mole fraction of menthol that was dissolved in SC-CO_2 which calculated by Soave-Redlich-Kwong equation of state (2.45E-02) and the actual mole fraction of menthol that put in the autoclave (2.40E-03).

Following **Figure 3.3**, it was clearly seen that menthol could dissolve into SC-CO_2. Hence, this work investigated the micronization of menthol at pre-expansion temperature 303, 313, 323 K, pre-expansion pressure 10,15 and 20 MPa and ethanol concentration 0, 10, 30 wt%, respectively that were shown in **Table 3.3**.

Table 3.3 Experimental conditions of micronized menthol

Parameters	Value
Pre-expansion temperature (K)	303, 313, 323
Pre-expansion pressure (MPa)	10, 15, 20
Ethanol concentration (wt%)	None, 10, 30

The fundamental knowledge about controlling morphology, particle size and particle size distribution of menthol were obtain from this part.

3.2.2 Estimation of PEG6000 solubility in carbon dioxide

For solubility of PEG6000, it could estimate from Sanchez-Lacombe equation, the calculation of PEG6000 solubility was shown in **Table 3.4** and **Figure 3.4**.

Table 3.4 Calculated mass fractions of CO_2 + PEG6000 + ethanol system at 20 MPa

	mass fraction of CO_2	mass fraction of PEG6000	mass fraction of ethanol
313 K	5.63E-01	6.50E-02	2.91E-01
	6.40E-01	3.51E-02	3.21E-01
	7.20E-01	1.32E-02	2.51E-01
	7.80E-01	5.00E-05	2.63E-01
323 K	mass fraction of CO_2	mass fraction of PEG6000	mass fraction of ethanol
	5.80E-01	7.74E-02	3.52E-01
	6.53E-01	5.04E-02	2.97E-01
	8.97E-01	5.80E-04	1.03E-01
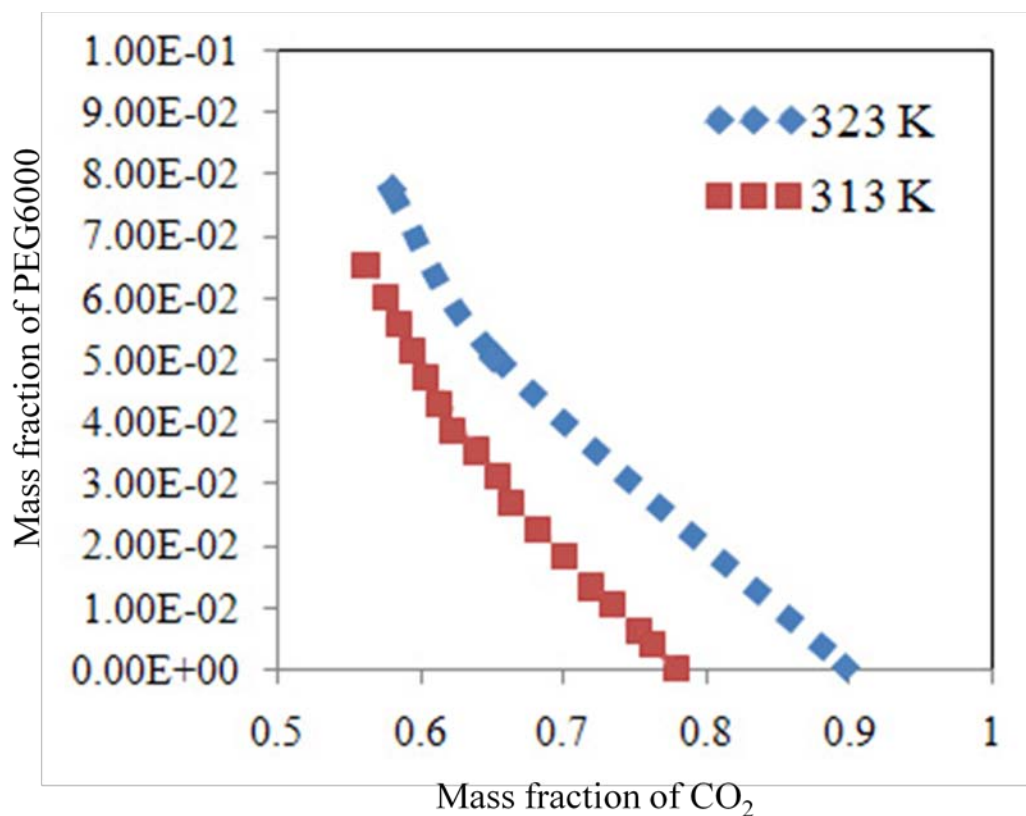
Figure 3.4 Estimation of solubility of PEG6000 at 20 MPa provided by Sanchez-Lacombe equation

The solubility behavior of PEG6000 in this system may be described as follows: Without PEG6000, the mixture of CO_2 and ethanol forms a single supercritical fluid phase. It can be clearly seen that PEG6000 does not dissolve in pure SC-CO_2. The solubility of PEG6000 is strongly dependent on the concentration of ethanol. The effect of ethanol concentration on the enhancement of PEG6000 solubility is observed in **Figure 3.4**. As a result of the phase equilibrium calculations, the suitable amount of ethanol concentration should be put in autoclave is 30 wt%. However, this study recommended to use ethanol in system was around 10 wt% due to avoid deformation of product. An increase in temperature and pressure can also help improve solubility of PEG6000. However, preliminary experimental result at 303 K showed that could not

found micronized PEG6000 same as pre-expansion pressure at 10 MPa. The results are consistent with the experimental result of Gupta, 2007. Therefore, this study investigates the effect of pre-expansion temperature at 313 and 323 K and pre-expansion pressure at 15 and 20 MPa. In summary, the experimental conditions of micronization of PEG6000 are shown in **Table. 3.5**.

Table 3.5 Experimental conditions of micronized PEG6000

Parameters	Value
Pre-expansion temperature (K)	313, 323
Pre-expansion pressure (MPa)	15, 20
Ethanol concentration (wt%)	10, 30

The amount of PEG6000 that was put in the autoclave should be less than amount of PEG6000 at equilibrium state provided by Sanchez-Lacombe equation of state. Then the phase composition of experiment was considered.

Table 3.6 Example of experimental condition of micronized PEG6000 at 313 K, 20 MPa, 30 wt% of ethanol

Substance	density (g/ml)	Flow rate (ml/min)	P (MPa) = 20 time (min)	T (K) = 313 mass (g)	weight fraction	mole fraction	Solubility of PEG6000 @313 K,20 MPa (mass fraction) provided by Sanchez-Lacombe EOS
CO$_2$	0.78	10	48	374.4	6.851E-01	7.028E-01	
Ethanol	247	volume (ml) 0.789		165.69	3.032E-01	2.971E-01	
Menthol				0	0.00E+00	0.00E+00	
PEG6000				6.4	1.17E-02	8.81E-05	3.51E-02

From **Table 3.6**, all of PEG6000 was dissolved into supercritical state observed by the mass fraction of PEG6000 that was dissolved in SC-CO_2 which calculated by Sanchez-Lacombe EOS (3.51E-02) and the actual mole fraction of PEG6000 that put in the autoclave (1.17E-02). Theoretically, PEG6000 should be dissolve in SC-CO_2 completely. The fundamental knowledge about controlling morphology, particle size and particle size distribution of PEG6000 were obtain from this part.

For four phase compositions (menthol + PEG6000 + ethanol + CO_2), the solubility of each solute had to ensure that all solute dissolved in SC-CO_2 completely by corresponding the solubility modeling of PEG6000 and the solubility modeling of menthol respectively. Referring to the fundamental knowledge about controlling morphology, particle size and particle size distribution of PEG6000. Both of knowledge from two parts would be adapted for the formation of encapsulated particle of menthol and PEG6000 to obtain the best condition for the experiment which is at pre-expansion temperature 323 K, pre-expansion pressure 20 MPa and ethanol concentration 10, 30 wt%, respectively.

Table 3.7 Experimental conditions of encapsulated particle of menthol and PEG6000

Parameters	Value
Pre-expansion temperature (K)	323
Pre-expansion pressure (MPa)	20
Ethanol concentration (wt%)	10, 30

3.3 Particle size, Morphology and Particle size distribution analysis

The images of the obtained product by Scanning electron microscope (SEM; E-SEM, FM3400, Hitachi) and Optical microscope (OM; OLYMPUS CX31) were

determined by image processing using Image Pro plus for particle size, morphology and particle size distribution.

Particle size characterization

Because the many kinds of product morphology were observed from the experiments, the projected area diameter (Heywood diameter) was chosen to describe the effect of RESS parameters on particle size and particle size distribution. The sample of original image was shown in **Figure 3.5.**
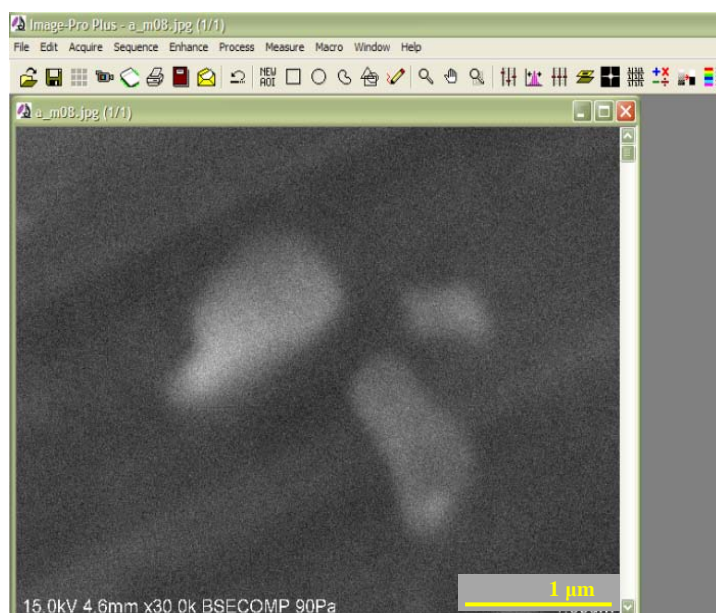
Figure 3.5 Original image before image processing`

Because the image was indistinct, color and contrast configuration were used to adjust it and then it was analyzed by Image Pro plus 6.0 for determining the Heywood diameter as shown in **Figure 3.6**.
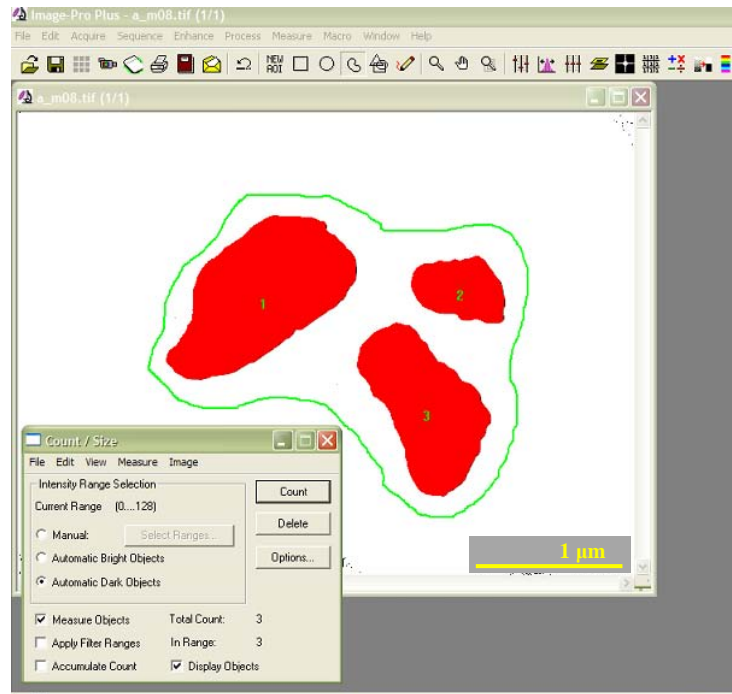
Figure 3.6 Determining particle size by image processing

The area of each particle was determined and exported to an Excel spreadsheet for Heywood diameter calculation as expressed in **Equation 2.36.**

$$d = \left(\frac{4A}{\pi}\right)^{1/2}$$
(2.36)

where d and A are Heywood diameter (μm) and projected area (μm^2)

The Heywood diameter was used as a tool to describe the effect of RESS parameters on particle size and particle size distribution.

CHAPTER IV

RESULTS AND DISCUSSION

4.1 Micronization of menthol

In reference to the many experimental results reported in previous studies, the aim of this section to examine the effects of RESS parameters, which are pre-expansion temperature (T_{pre}), pre-expansion pressure (P_{pre}), ethanol concentration on morphology, particle size and particle size distribution, which are the experimental conditions outlined in **Part 3.2.2**. The fundamental knowledge about controlling morphology, particle size and particle size distribution of menthol were obtained in order to use as a guideline for experimental condition setting of PEG6000 and the encapsulated particle of menthol and PEG6000. About experimental conditions were shown in **Table 3.3**

4.1.1 Effect of ethanol concentration on morphology, particle size and particle size distribution.

Ethanol has been widely used to increase solubility of solute in RESS process. It should be affected on morphology and size of product particle due to its properties. Therefore, this study investigated the effect of ethanol on morphology and size of particle.

The morphology at various ethanol concentrations were shown in **Figure 4.1**
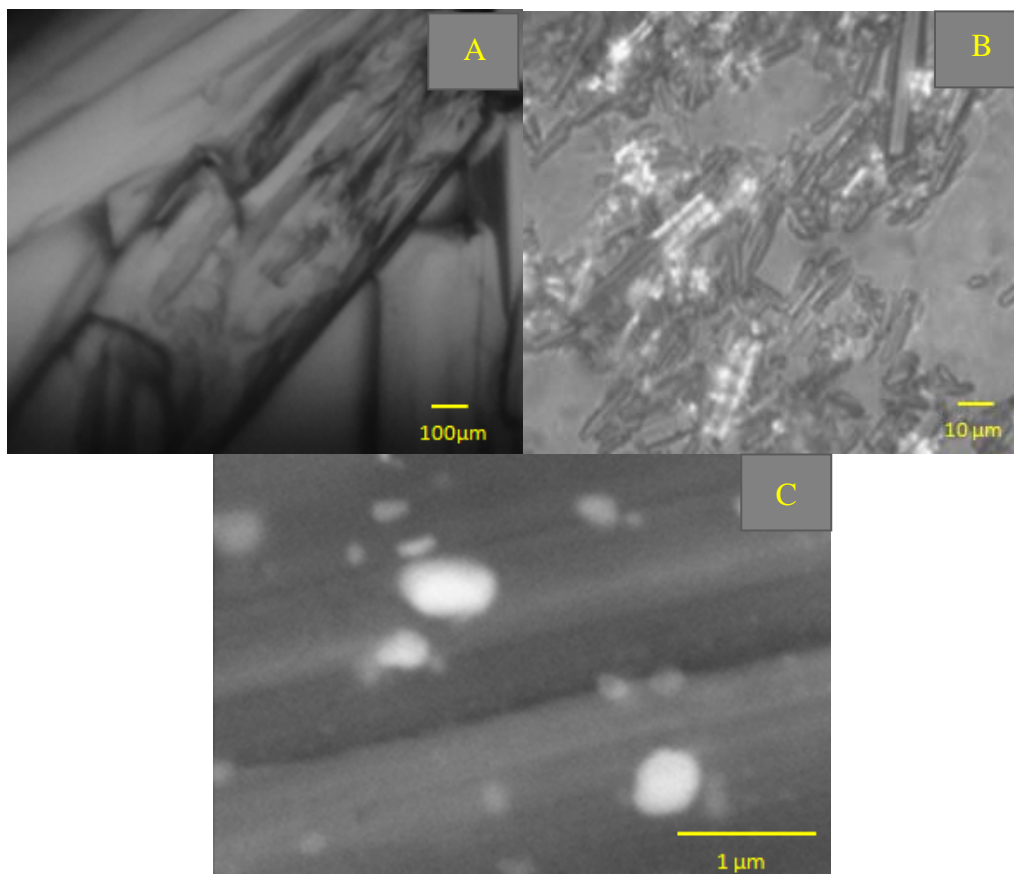
Figure 4.1 Morphology of menthol (A) unprocessed menthol (B) at 10 MPa, 303 K without ethanol and (C) at 10 MPa, 303 K with 10 wt% of ethanol.

The morphology changed from needle-like to rod-like and almost circle when increasing the amount of ethanol, respectively. Furthermore, the particle size and geometric standard deviation at various ethanol concentrations were also investigated as shown in **Figure. 4.2** and **Figure 4.3**, respectively.
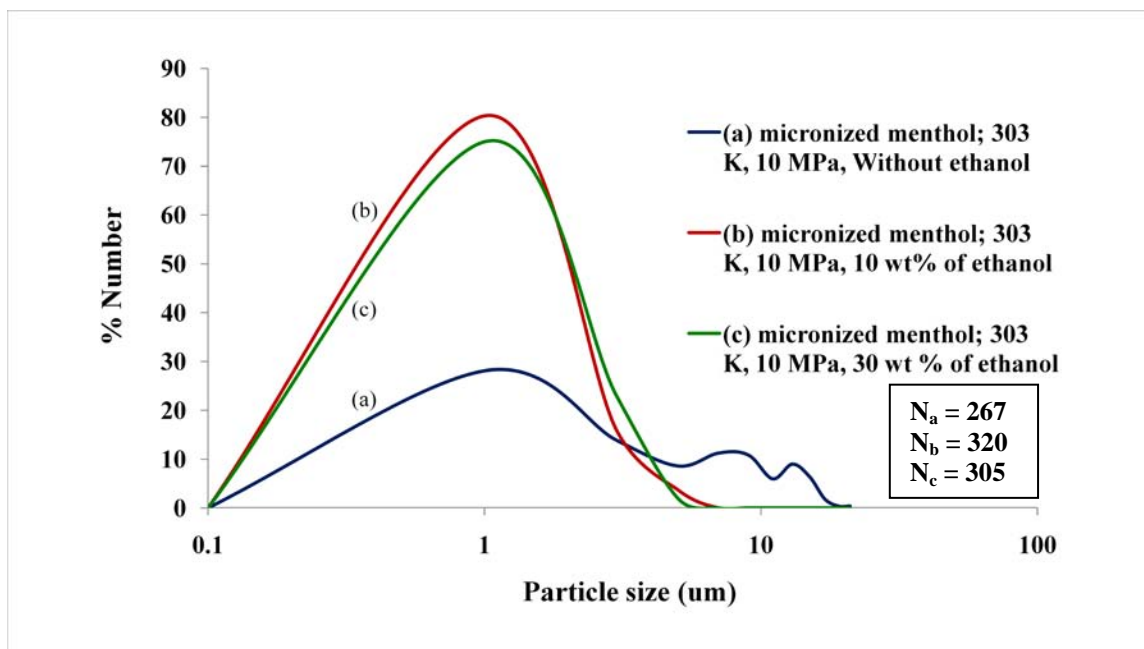
Figure 4.2 PSD of obtained menthol at 303 K, 10 MPa with different ethanol concentration
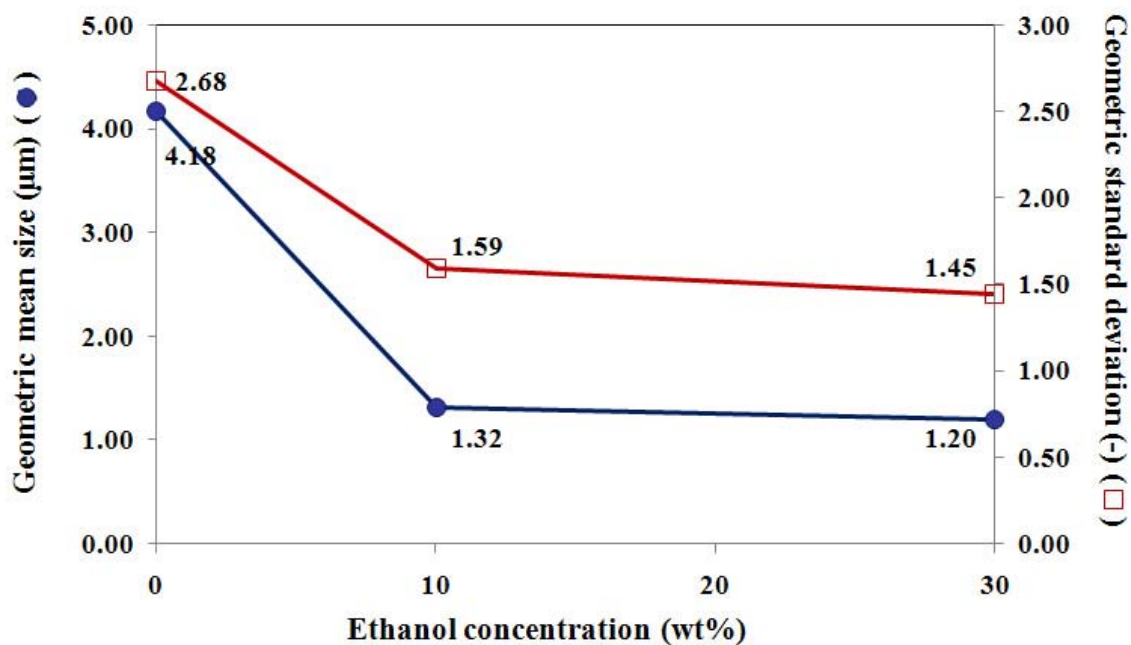
Figure 4.3 Geometric mean size and standard deviation of obtained menthol at 303 K, 10 MPa with different ethanol concentration

At low solubility of menthol in SC-CO_2 for the solution inside autoclave, it led to high degree of supersaturation at the edge of nozzle when spraying. Solvent diffused out the solution rapidly caused to be fast nucleation rate and low opportunity to occur surface integration. Thus the large amount of fine particle should be obtained. On the other hand, high solubility of menthol led to low degree of supersaturation at the edge of nozzle. Solvent gradually diffuse out the solution caused to be slow nucleation rate and high opportunity to occur surface integration. Thus the bigger particles were obtained. The phenomenon were shown in **Figure 4.4**
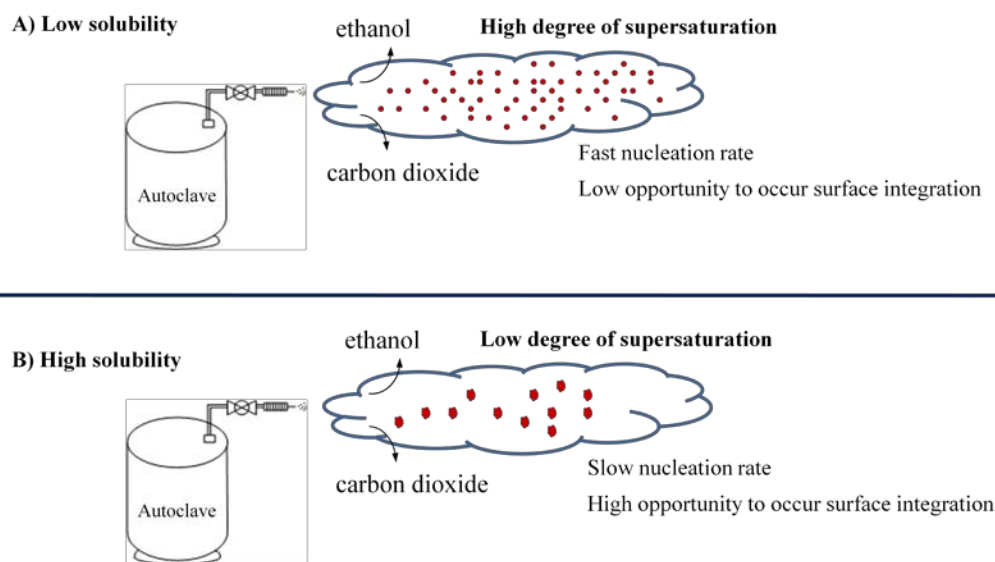
Figure 4.4 Phenomenon of particle formation by RESS-CO_2 with ethanol as co-solvent

However, ethanol had also effected on morphology and size. Therefore, the smaller particle size were obtained when increase in ethanol concentration that were shown in **Figure 4.3**. The explanation of morphology and size were also investigated in this study.

Uchida et al., (1990) found that the growth mechanism in the supercritical phase was the same as in the liquid or gas phases, and the growth kinetics was intermediate between those in a liquid and in gas. To investigate the effect of ethanol concentration on

morphology and particle size of menthol, a set of crystallization experiments were carried out. Both of menthol and ethanol were put into the liquid phase by heating with hot plate at 313 K and then the solutions of menthol and ethanol were titrated with different concentrations that were shown in **Figure 4.5**.
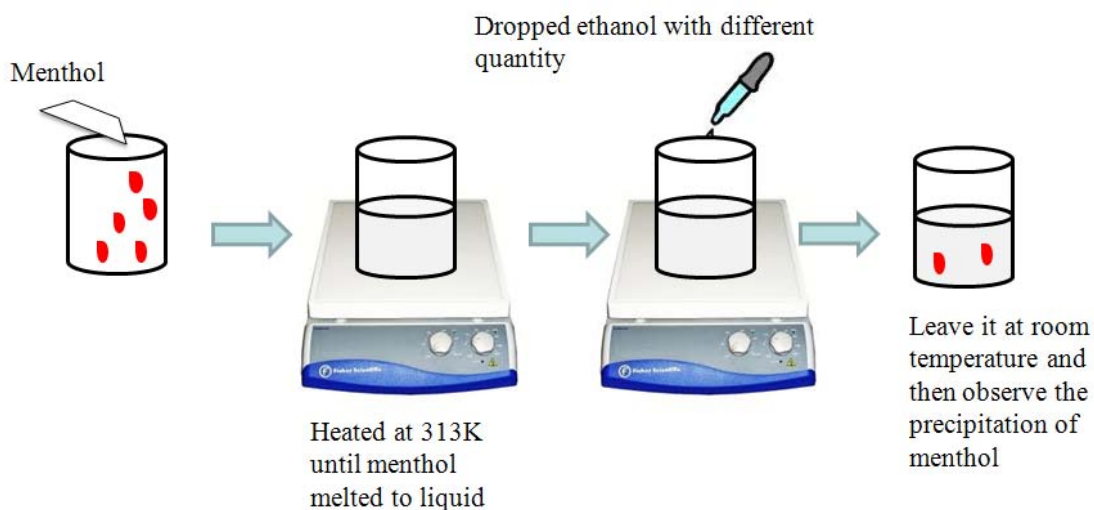
Figure 4.5 Preparation of menthol crystallization in liquid phase

The density of menthol crystals in vivo were examined by visual as shown in **Figure 4.6**.
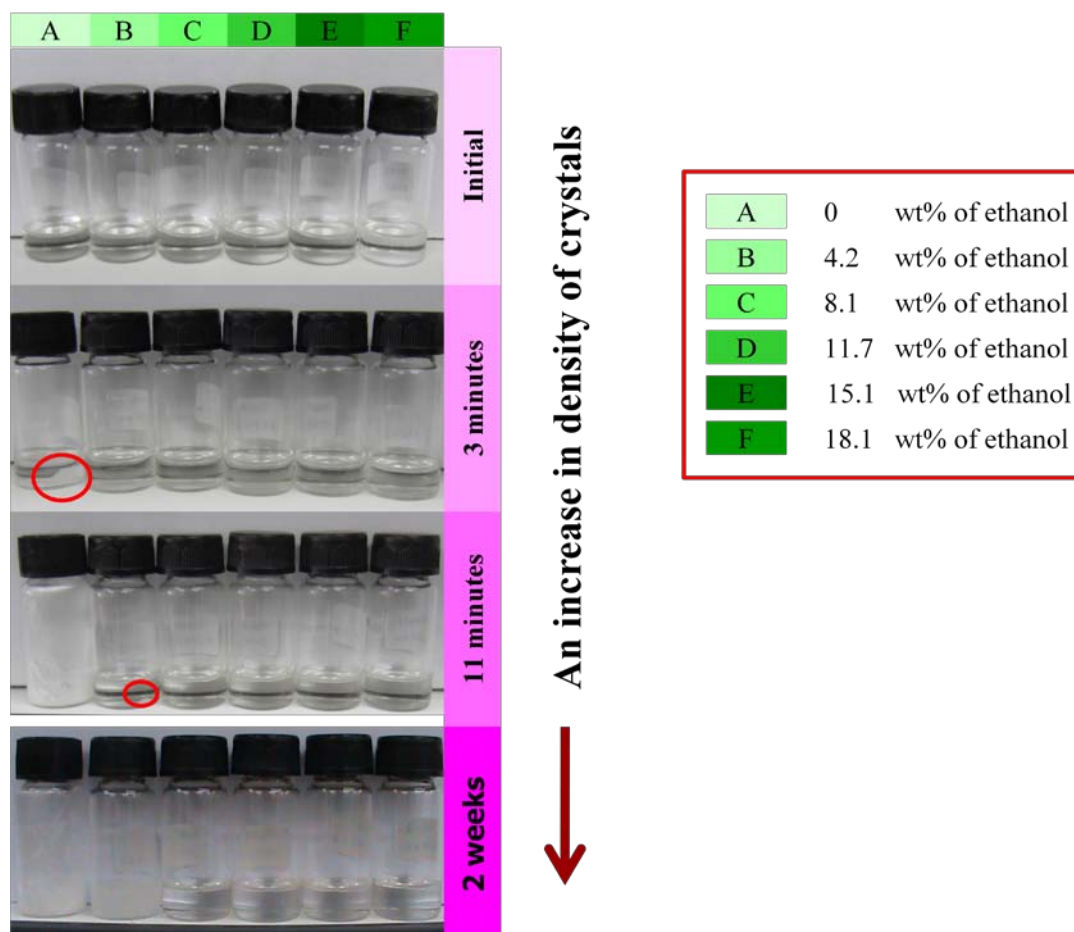
Figure 4.6 Crystallization of menthol in liquid phase at different ethanol concentration.

As shown in **Figure 4.2,** this study found that adding some ethanol caused to a slow nucleation rate and growth rate (the red circle showed the time that solid phase occurred and the tendency of density increased over time by visual observation). Because surface integration of crystal was being held back by ethanol due to they are different crystallographic faces of crystal. Ethanol was impurity or additives in menthol crystallization system. The effect of impurity is generally thought to result from adsorption on the surface of the growing crystal. Sincerely, adsorption has two effects. It generally decreases the interfacial tension, thus resulting in greater surface nucleation in the birth and spread mode of growth. On the other hand, impurity adsorption will block

growth sites, thus reducing growth rate in both modes of growth. Moreover, solubility was also affected by impurity, increase in solubility will result a decrease in degree of supersaturation and thus apparent reduce growth rate. Hence, ethanol behavior liked the second effect (Davey., 1979 and D. Randolph., 1988).

This study also investigated the product yield. The definition of product yield in this study was shown in **Equation 4.1**

$$Product\ yield\ (\%) = \frac{Mass\ of\ ment\ hol\ in\ collecting\ chamber\ (g)}{Total\ mass\ of\ ment\ hol\ (g)} \times 100(\%) \qquad (4.1)$$

The amount of obtained menthol with different ethanol concentrations were shown in **Figure 4.7.**
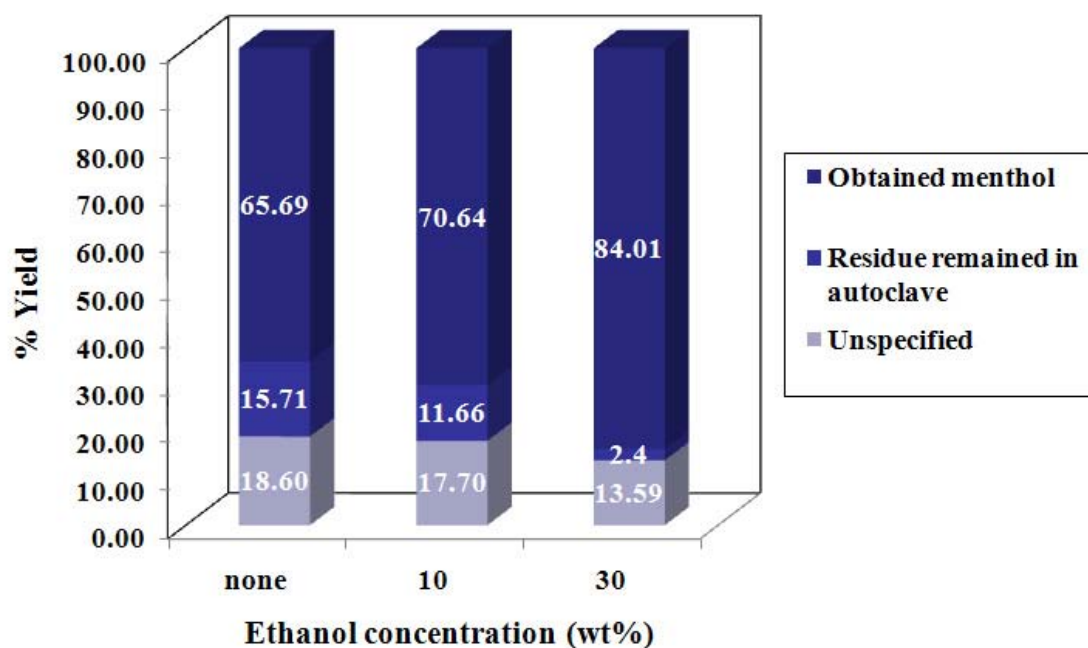
Figure 4.7 Effect of ethanol concentration 313 K, 10 MPa with different ethanol concentration on %yield of menthol

Adding small amounts of polar compounds as co-solvents, entrainers or modifiers to CO_2 could enhance the solubility of polar and non-polar solutes in SC-CO_2. Water and

short-chain alcohols are usually the most acceptable co-solvent in industrial. However, the solubility of menthol in CO_2 will decrease when adding amount of ethanol too much theoretically. As mention earlier, ethanol could reduce the interfacial tension resulting better nucleation and surface integration. Thus the large amount of menthol was obtained. About the amount of residue, there is some remained menthol due to the equipment could not push the product out of the autoclave completely. An unspecified amount of menthol was menthol that might pass through HEPA filter or remain in the collecting chamber. This study used THF (Tetrahydrofuran) solvent to dissolve menthol in both autoclave and collecting chamber after that used TGA; thermo-gravimetric/differential analyzer (TG/DTA; TGA/SDTA 851^e, Mettler Toledo, Switzerland) to identify total amount of menthol in the solution. The details of TGA also showed in **Appendix A**.

4.1.2 Effect of pre-expansion temperature on morphology, particle size and particle size distribution

Pre-expansion temperature was main factor for RESS operation because it related to solubility of solute (menthol). Thus effect of temperature was investigated in this study. The particle size distribution, geometric particle size and standard deviation were investigated as shown in **Figure 4.8** and **Figure 4.9**, respectively.
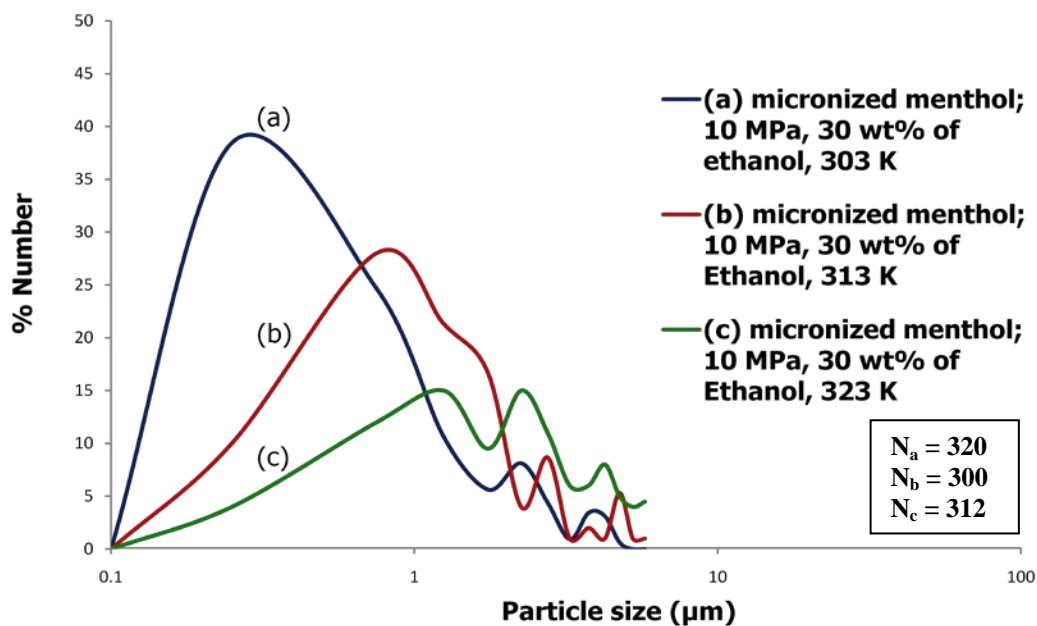
Figure 4.8 PSD of the obtained menthol at 10 MPa, 30 wt% of ethanol with different temperature

Figure 4.9 Geometric mean size and standard deviation of obtained menthol at 10 MPa, 30 wt% of ethanol concentration with different pre-expansion temperature

As results shown in **Figure 4.9**, the tendency of particle size rose up when an increase in temperature. As mentioned earlier, the particle size was increased due to high solubility of menthol in autoclave and then when spraying, the degree of supersaturation would be low resulting bigger formulated particles obtained. Additionally, temperature also affected on growth mechanisms. After nuclei appearance, the velocity of particle was depended on temperature profile of spraying. This was a reason why particle may coagulation and condensation during spraying. Thus the products might be bigger than normal situation that was proven by **Figure 4.10**.
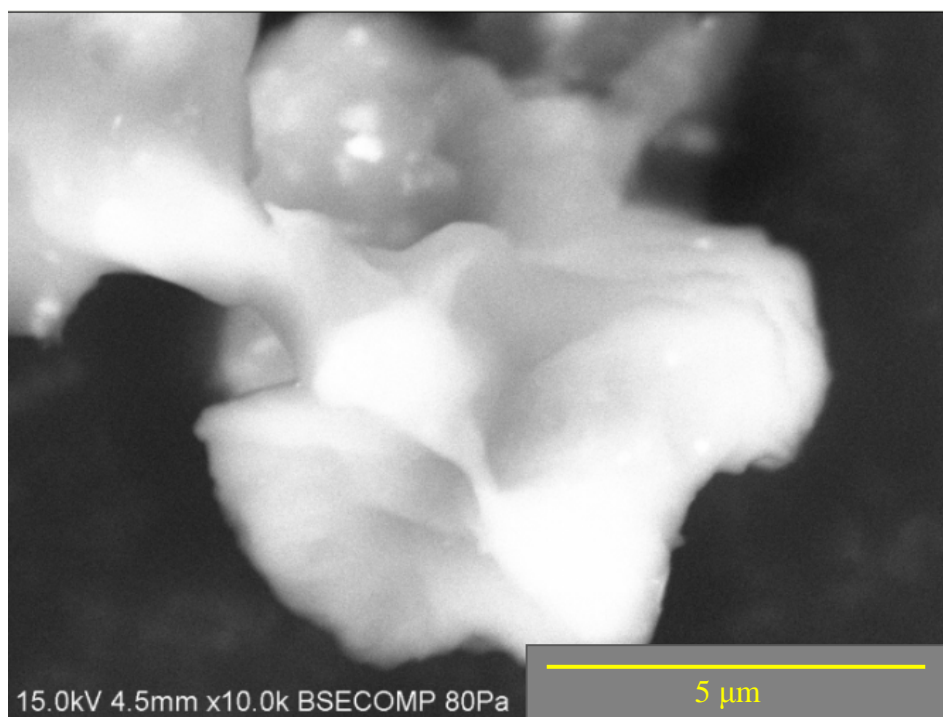
Figure 4.10 SEM image of the obtained menthol showing the coagulation and condensation of the obtained particles at 10 MPa, 10 wt% of ethanol, 323 K

At 323 K, the particle might be coagulation and condensation resulting a greater possibility of particles merging and collision each other. Thus the particle size was bigger. However, this study put some ethanol into the experiment due to good results on

Part 4.1.1. Ethanol still controlled the standard deviation of particles. Therefore, an increase of temperature did not affect significantly on the standard deviation of particle size distribution.

The amount of the obtained menthol at different pre-expansion temperature were shown in **Figure 4.11**
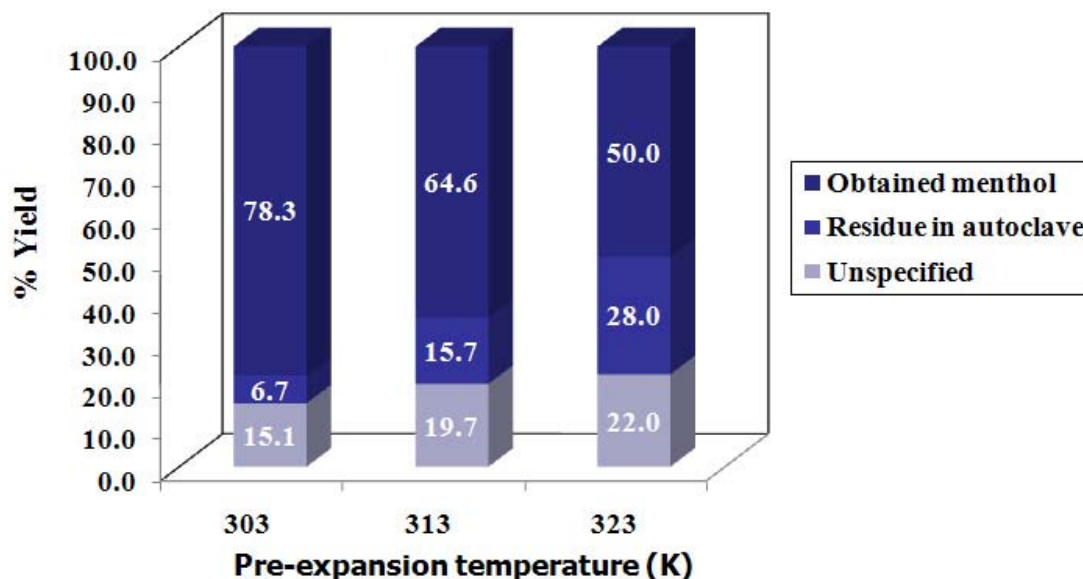
Figure 4.11 Effect of pre-expansion temperature at 10 MPa, none ethanol concentration with different temperature on % yield of menthol

From **Figure 4.11** showed that higher pre-expansion temperature was lower % yield than lower pre-expansion temperature and the amount of residue also increased significantly. This might be caused of low solubility of menthol in SC-CO_2 at 10 MPa when increasing temperature as mentioned earlier in **Figure 3.3**.

4.1.3 Effect of pre-expansion pressure on morphology, particle size and particle size distribution.

Pre-expansion pressure was also main factor for RESS operation because it related to solubility of solute (menthol). Thus effect of pressure was investigated in this study. The morphology, particle size distribution, geometric particle size and standard deviation were investigated as shown in **Figure 4. 12**, **Figure 4.13** and **Figure 4.14**, respectively.
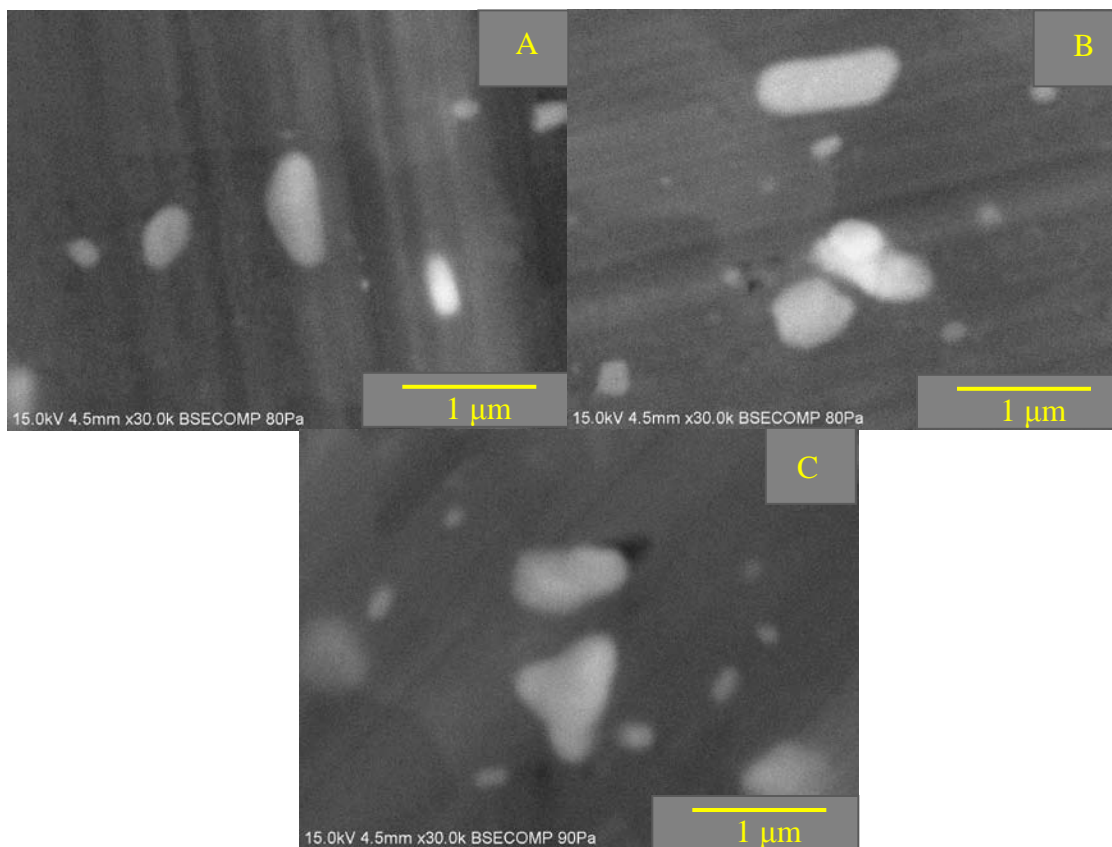

Figure 4.12 SEM image of menthol with constant pre-expansion temperature 323 K and 30 wt% of ethanol; (A) with pre-expansion 10 MPa, (B) with pre-expansion 15 MPa and (C) with pre-expansion 20 MPa

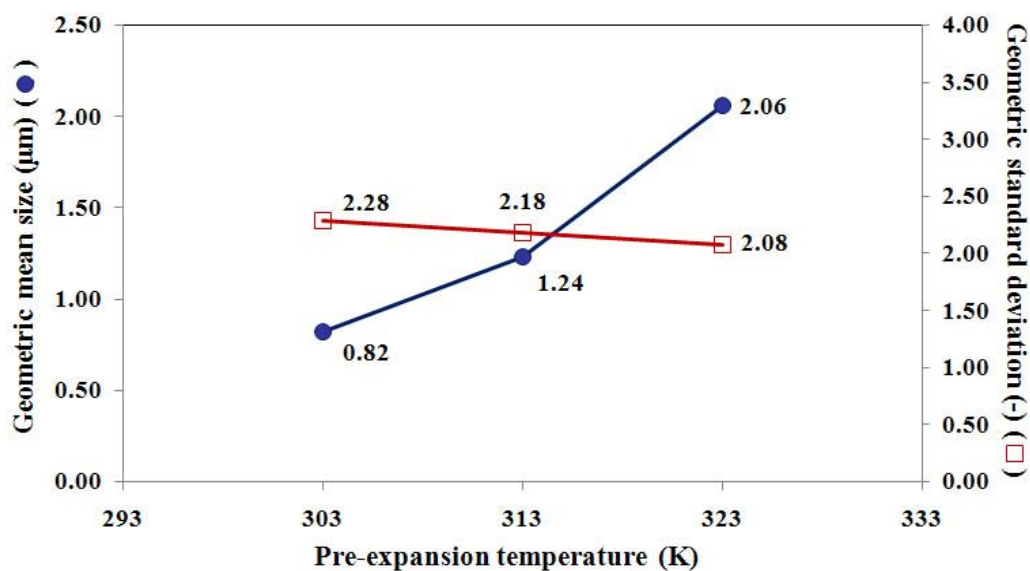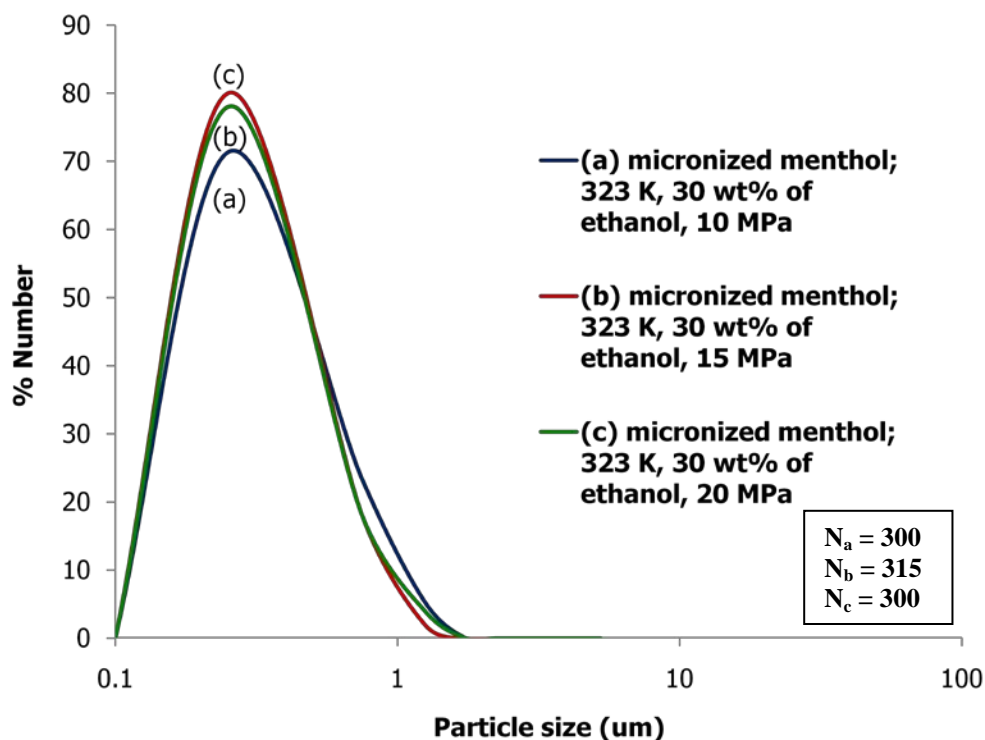**Figure 4.13** PSD of the obtained menthol at 323 K, 30 wt% of ethanol concentration with different pressure

Figure 4.14 Geometric mean size and standard deviation of obtained menthol at 323 K, 30 wt% of ethanol concentration with different pre-expansion pressure

An increase in pressure led to be higher solubility of menthol in SC-CO$_2$ as mentioned earlier in **Figure 3.3.** However **Figure 4.12** - **Figure 4.14** showed that the pre-expansion pressure had small influence on morphology and particle size distribution but the results showed that the obtained particles were in the range of nanometer and submicron as well. Adding high ethanol concentration may be the reason of the phenomena as mentioned earlier. Therefore, this study could conclude the potential of the effect of ethanol concentration, pre-expansion temperature and pre-expansion pressure on micronized menthol as below.

Pre-expansion pressure < Pre-expansion temperature < Ethanol concentration

The amount of the obtained menthol at different pre-expansion pressures was shown in **Figure 4.15.**
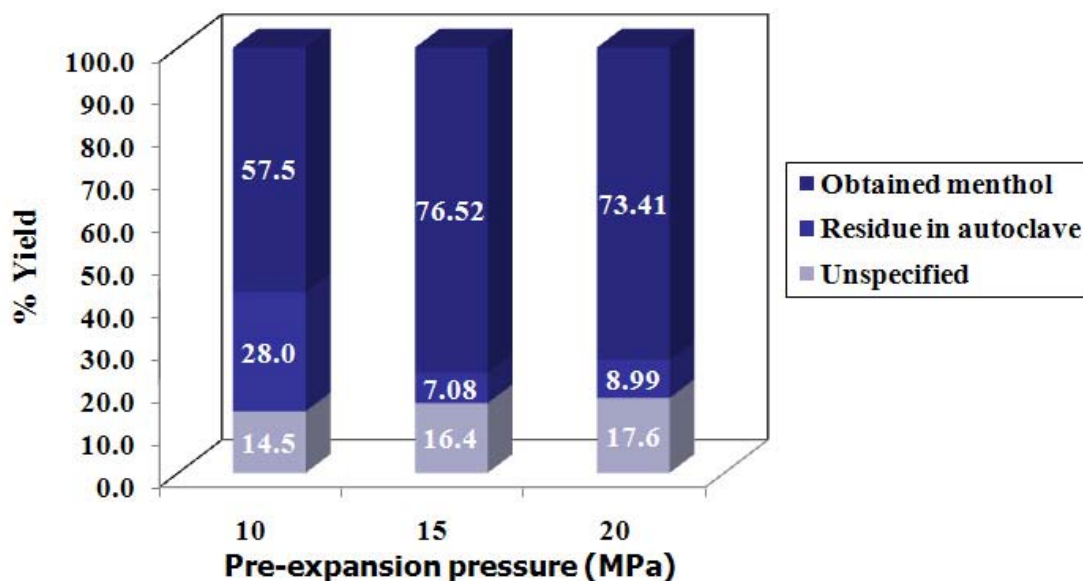
Figure 4.15 Effect of pre-expansion pressure 303 K, 10 MPa with different ethanol concentration on %yield of menthol

Figure 4.14 showed that increasing of pre-expansion pressure led to obtaining higher % yield. Because at higher pre-expansion pressure, solubility of menthol increased as shown in **Figure 3.3** and the force to push product out of the autoclave also increased that why the large amount of product was obtained.

4.1.4 Examining the chemical characteristic of the obtained particle.

The obtained particles were analyzed by Fourier Transform Infrared Spectrophotometer (FT-IR) to check their chemical characteristic compared with the unprocessed menthol in order to ensure that the RESS process did not change chemical characteristic by checking chemical bonding and functional group of the sample. The results were show in **Figure. 4.16.**
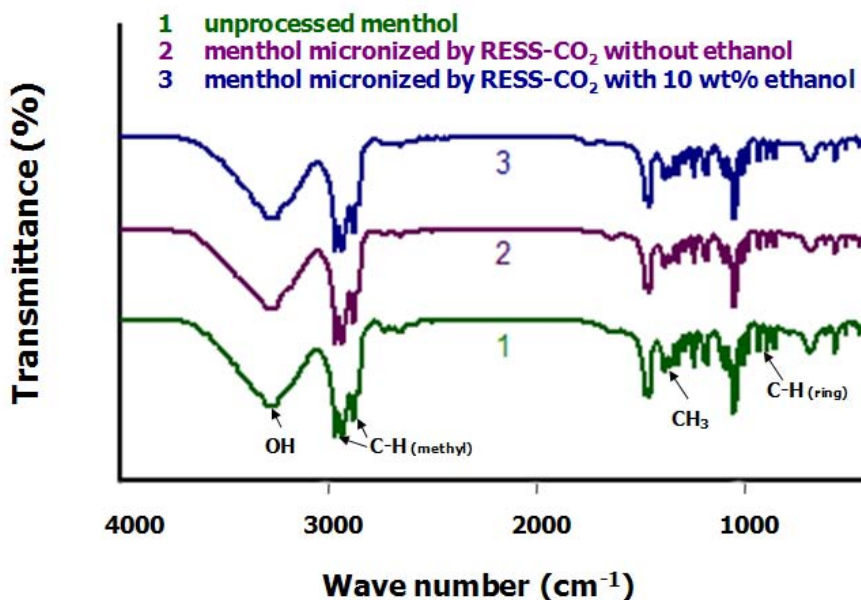
Figure 4.16 Fourier transform infrared spectroscopy of unprocessed menthol and menthol micronized by RESS-CO_2

From **Figure 4.16**, it was obvious that all of functional group still remained on the micronized menthol by RESS-CO_2 even adding some amount of ethanol in the experiments.

4.2 Micronization of PEG6000

According to **Part 4.1**, this study found that adding ethanol could help improve geometric mean particle size and standard deviation of micronized menthol. PEG6000 itself had low limitation to dissolve into SC-CO$_2$. Adding some ethanol also enhanced solubility of PEG6000 as shown in **Figure 3.4**. Adjusting pre-expansion temperature and pressure related to solubility of PEG6000 as well.

Hence, the effects of ethanol concentration, pre-expansion temperature and pre-expansion pressure were investigated. Understanding fundamental knowledge about controlling morphology, particle size and particle size distribution of PEG6000 would be useful for RESS process operation.

The experimental conditions also were shown in **Table 3.5**

4.2.1 Effect of pre-expansion temperature on morphology, particle size and particle size distribution.

Pre-expansion temperature related to the dissolution of PEG6000 in SC-CO$_2$. Adjusting temperature might be caused of the difference in morphology and particle size.

Because PEG6000 has limitation to dissolve into SC-CO$_2$.Ethanol adding was necessary. At low pre-expansion temperature (303K), this work could not detected amount of PEG6000. Furthermore, %yield of PEG6000 was also very low. It was difficult to determine the amount of PEG6000 with high accuracy. The researcher was reluctant to neglect %yield results. However, the results of were still consistent with Gupta and Shim 2007. The morphology, particle size distribution, geometric mean particle size and standard deviation were shown in **Figure 4.17**, **Figure 14.18** and **Figure 14.19**, respectively.

Figure 4.17 SEM image of micronized PEG6000 at 15 MPa, 10 wt% of ethanol concentration A) 313 K, B) 323 K

Figure 4.18 PSD of micronized PEG6000 at 15 MPa, 10 wt% of ethanol concentration with different pre-expansion temperature
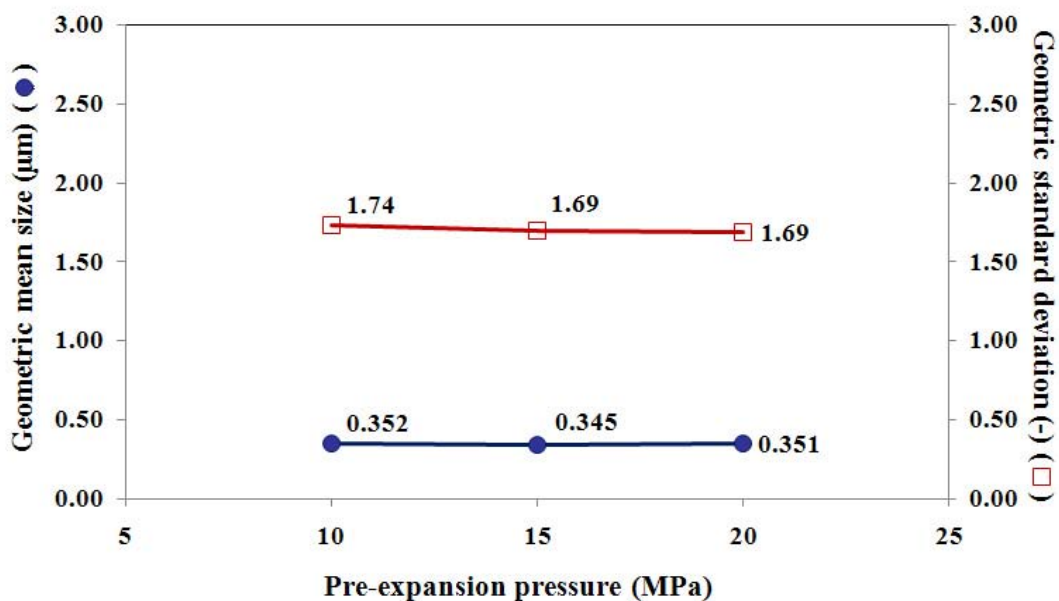
Figure 4.19 Geometric mean size and standard deviation of micronized PEG6000 at 15 MPa, 10 wt% of ethanol concentration with different pre-expansion temperature

From **Figure 4.17** – **Figure 4.19,** there were two type of micronized PEG6000 morphology, rod-like and almost circle. The mean particle size increased a little when temperature was risen because of high solubility in autoclave. Thus low degree of saturation occurred at the edge of nozzle. Hence, faster nucleation rate and high opportunity to be growth at the surface of particle resulting bigger particle size was obtained. However, ethanol might be obstructed the growth rate of particle and caused to get high possibility of rod-like and almost circle in morphology. Moreover, geometric standard deviation was also narrow.

4.2.2 Effect of pre-expansion pressure on morphology, particle size and particle size distribution.

Due to the limitation of PEG6000 dissolution in SC-CO$_2$, at low pre-expansion pressure (10 MPa), this work could not detected amount of PEG6000.

The morphology, particle size distribution, geometric mean size and standard deviation were shown in **Figure 4.20, Figure 4.21 and Figure 4.44**

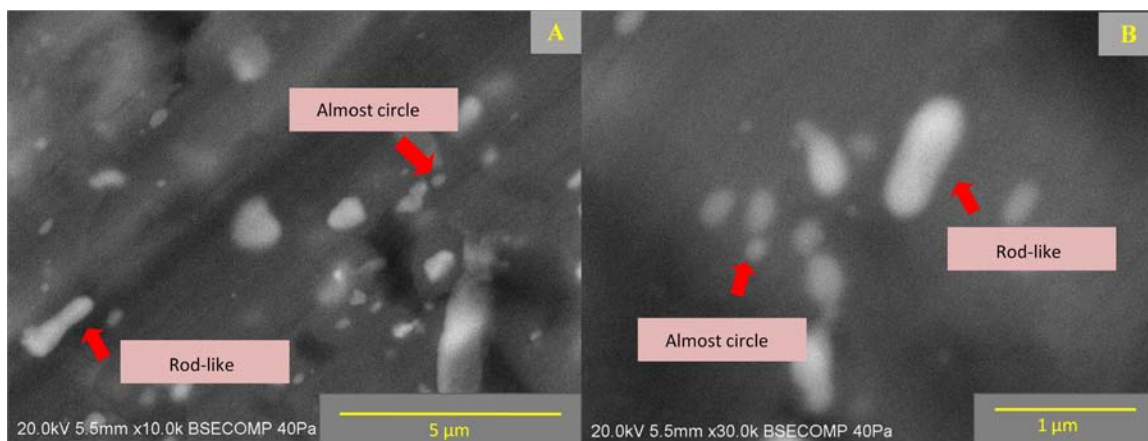
Figure 4.20 SEM image of micronized PEG6000 at 323K, 10 wt% of ethanol concentration A) 15 MPa, B) 20 MPa
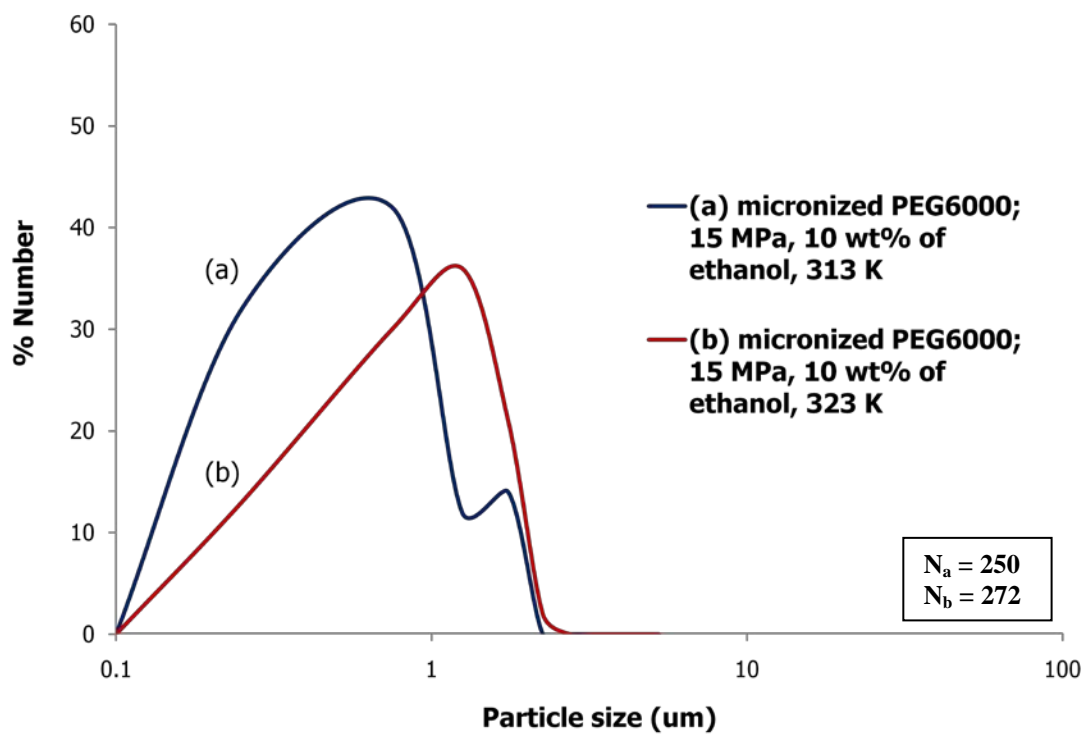
Figure 4.21 PSD of micronized PEG6000 at 323 K, 10 wt% of ethanol concentration with different pre-expansion pressure
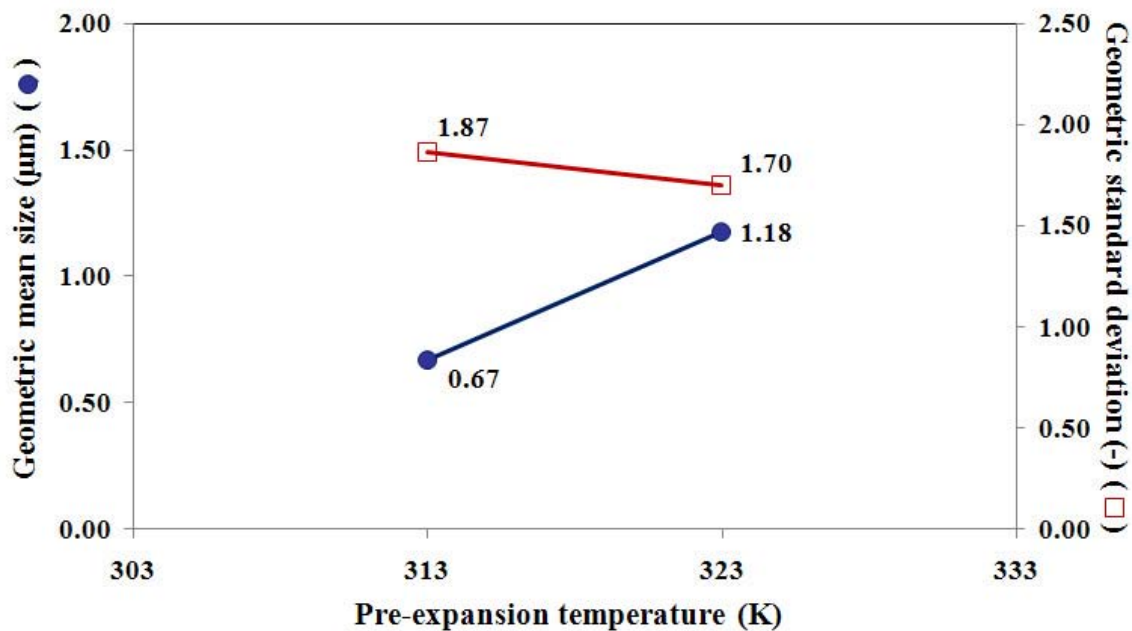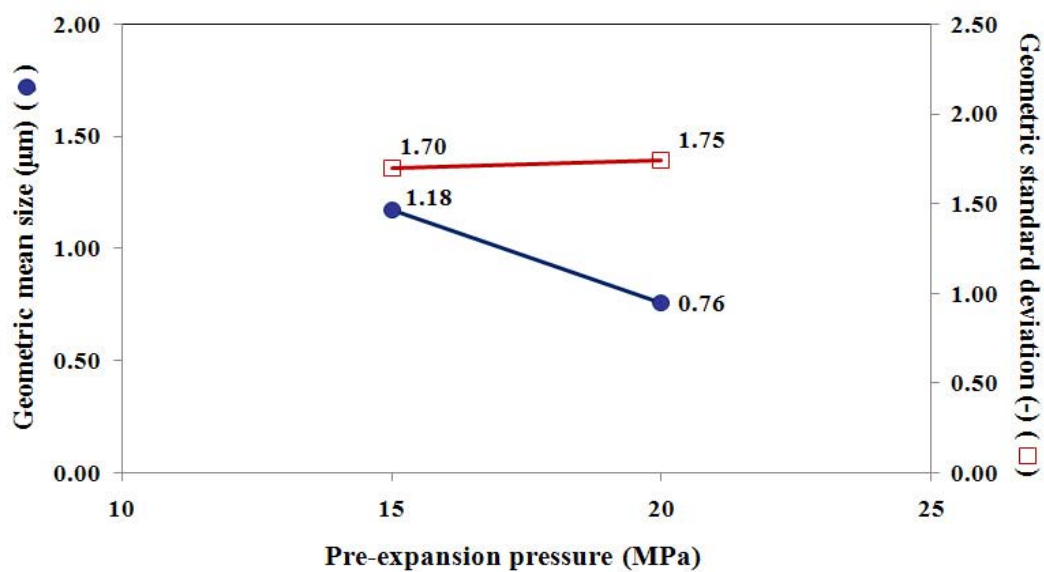

Figure 4.22 Geometric mean size and standard deviation of micronized PEG6000 at 323 K, 10 wt% of ethanol concentration with different pre-expansion pressure

From **Figure 4.20, Figure 4.21 and Figure 4.22**, there were two type of morphology similar to the effect of pre-expansion temperature. The micronized PEG6000 tended to be smaller particle size. Theoretically, an increase in pressure led to solubility in autoclave. Thus high degree of saturation occurred resulting bigger particle were obtained. However, the disruption of growth site due to ethanol also affected on morphology and particle size. Thus smaller particle size was produced and more possibility to get rod-like and almost spherical in morphology.

4.2.3 Effect of ethanol concentration on morphology, particle size and particle size distribution

Due to limitation of PEG6000 solubility in CO_2, co-solvent like ethanol was necessary. Ethanol could slightly improved PEG6000 solubility in CO_2 because ethanol improved polar interaction of solute and CO_2 (Liu et al., 2000, Jin et al., 2004).

The morphology, particle size distribution, geometric mean size and stand deviation were shown in **Figure 4.23, Figure 4.24 and Figure 4.25**
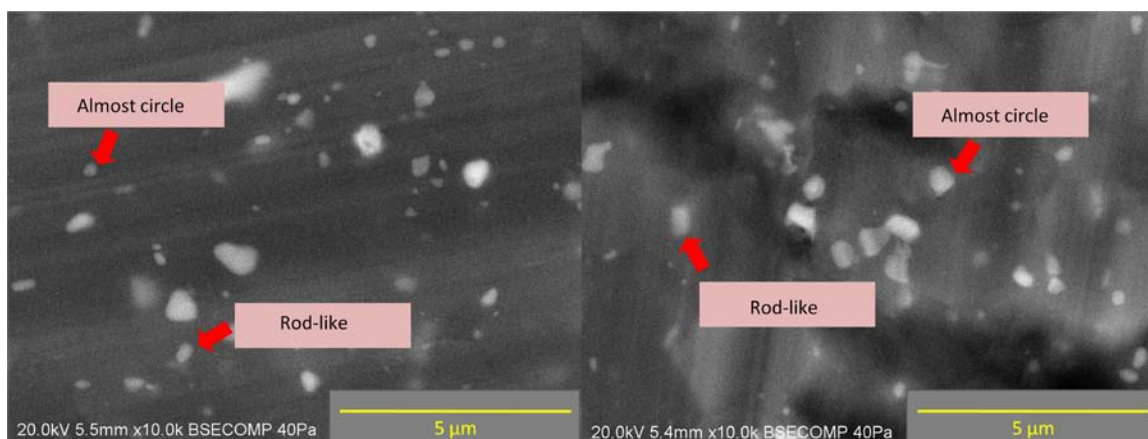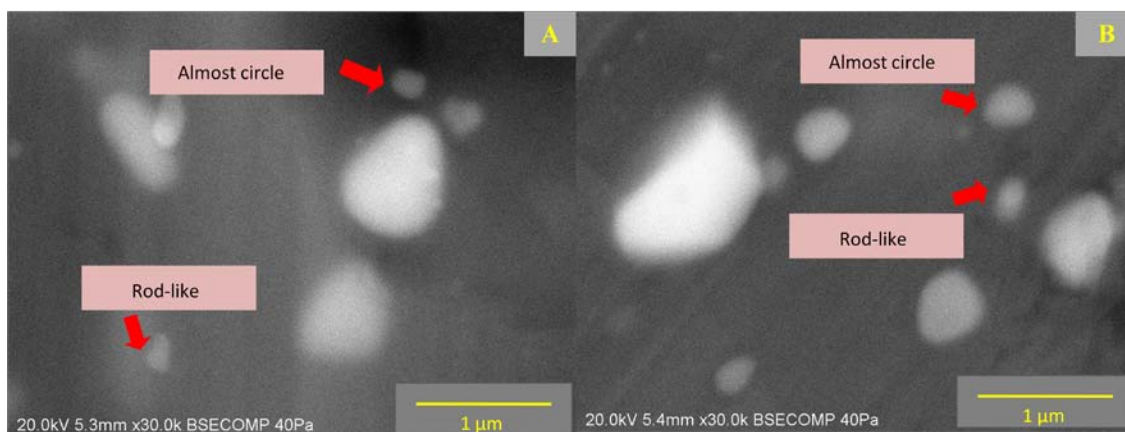

Figure 4.23 SEM image of micronized PEG6000 at 323K, 10 wt% of ethanol concentration A) 15 MPa, B) 20 MPa

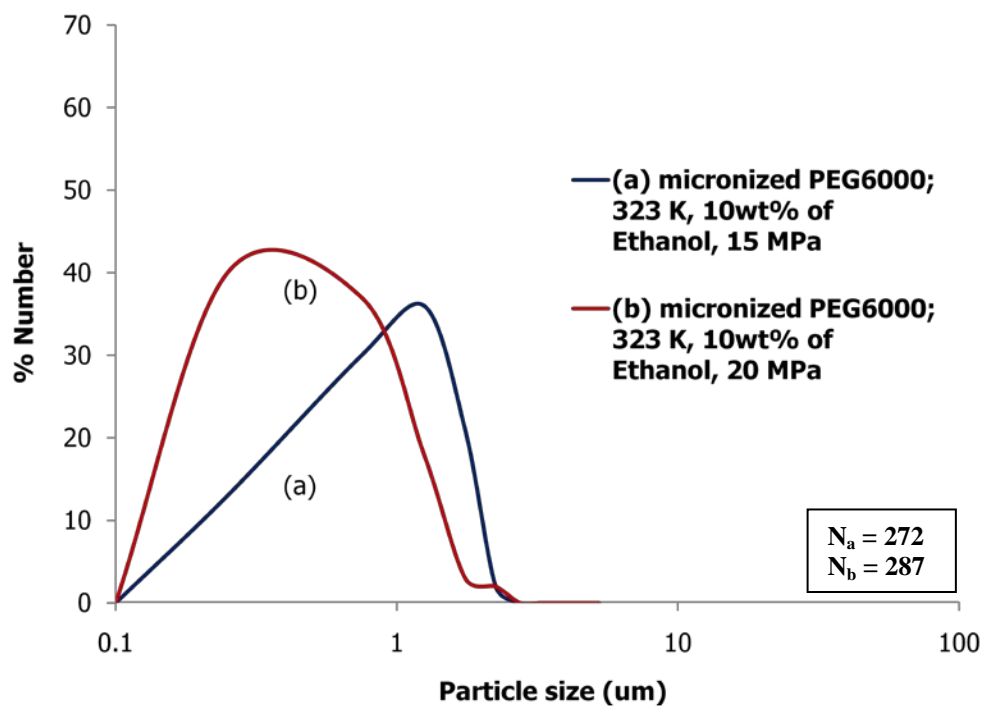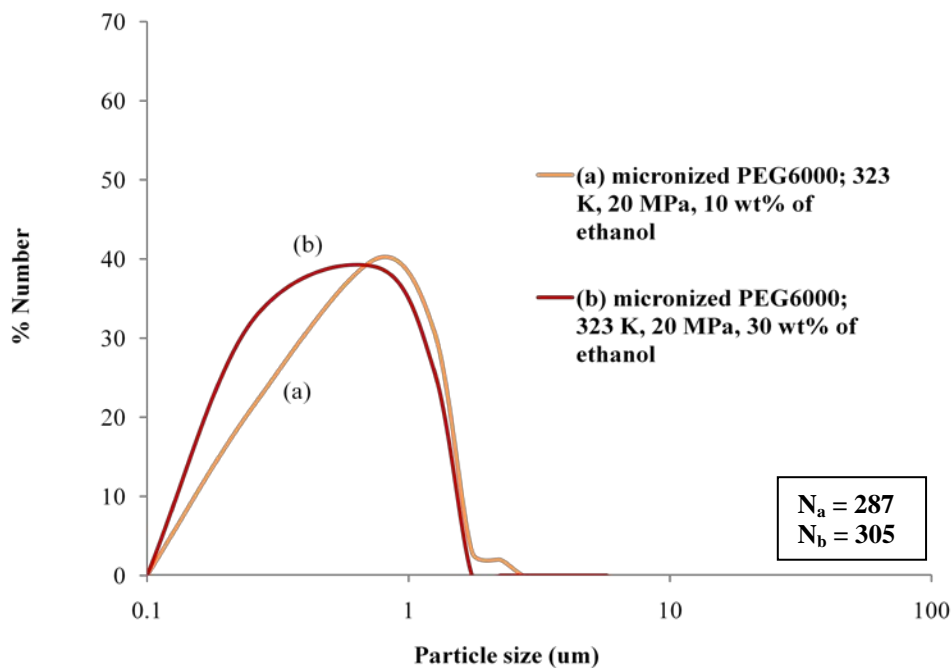**Figure 4.24** PSD of micronized PEG6000 at 323 K, 20 MPa with different ethanol concentration
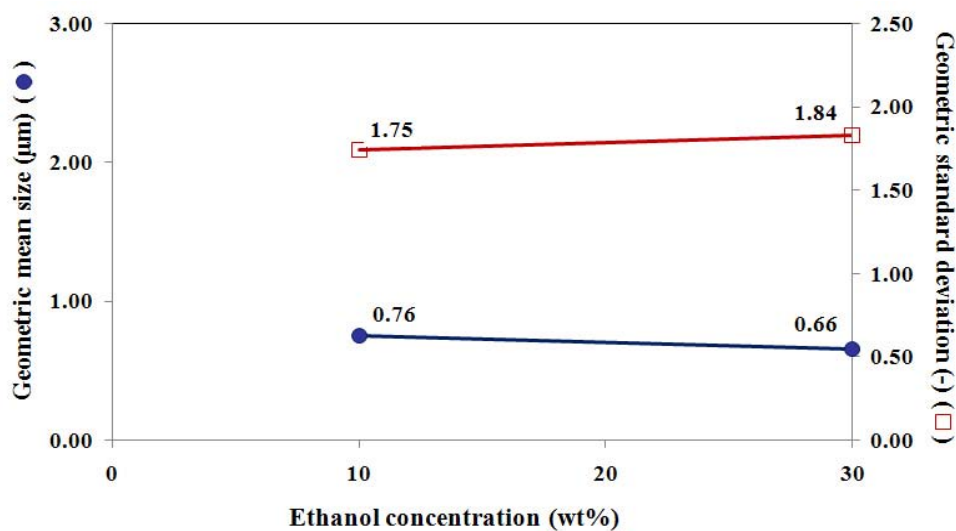
Figure 4.25 Geometric mean size and standard deviation of micronized PEG6000 at 323 K, 20 MPa with different ethanol concentration

Following **Figure 4.23, Figure 4.24** and **Figure 4.25**, because micronized PEG6000 required some amount of ethanol. Therefore, the morphology of micronized PEG6000 was rod-like and almost circle. The pre-expansion pressure did not affect on geometric mean size and standard deviation significantly. The geometric mean size was small because ethanol impeded the nucleation and growth rate as well. To investigate the effect of ethanol concentration on nucleation and growth rate. the set of crystallization experiments were carried out. Both of PEG6000 and ethanol were liquid phase by heating with hot plate at 313 K and then titrate the solutions of PEG6000 and ethanol with different concentration as shown in **Figure 4.26**
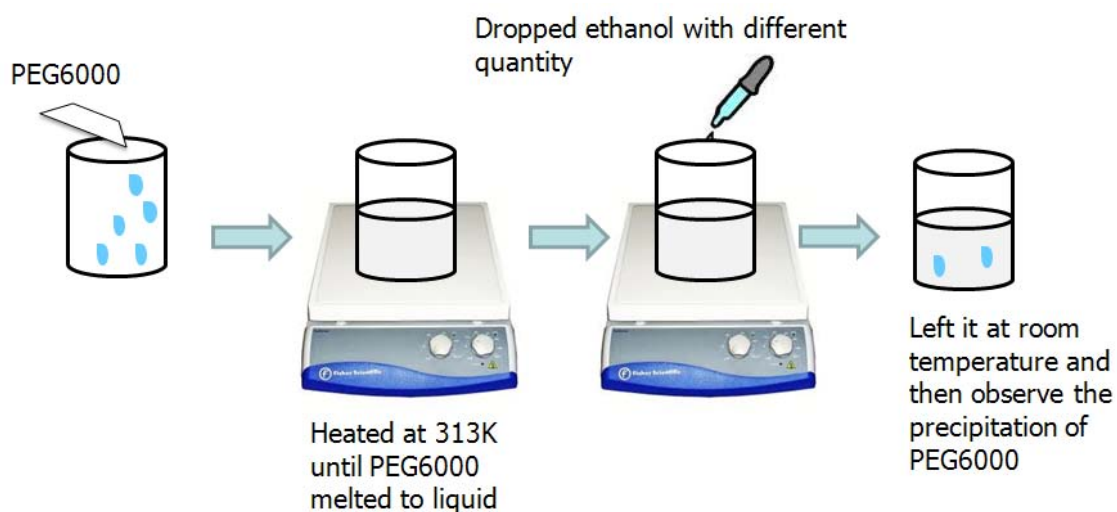
Figure 4.26 Preparation of PEG6000 crystallization in liquid phase

After finished preparation of solution, the experiment was observed the density of PEG6000 crystals in vivo by visual that was shown in **Figure 4.27.**
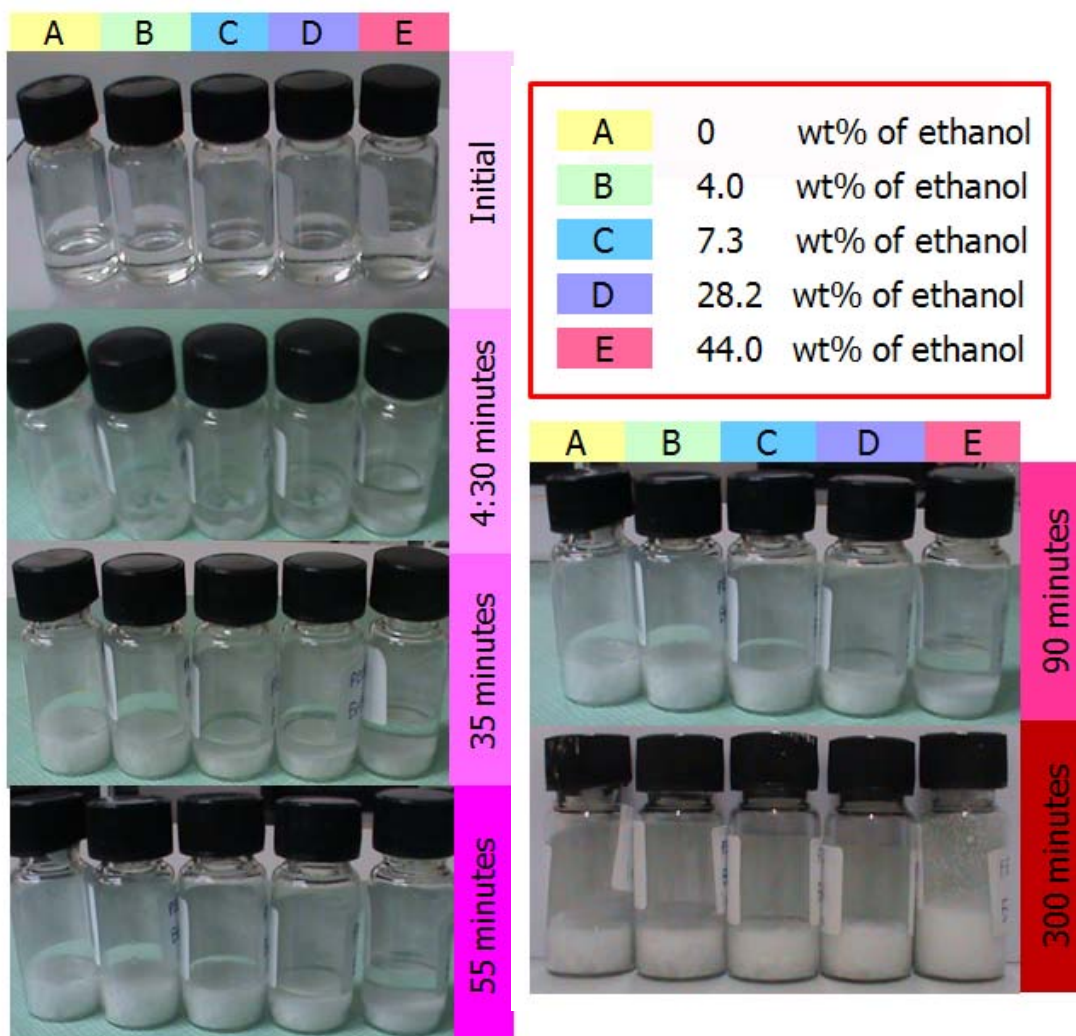
Figure 4.27 Crystallization of PEG6000 in liquid phase at different ethanol concentration

As results from **Figure 4.27**, all of samples precipitated around the minute of 4.30 with the different amount of PEG6000 crystals observed by visual and then the PEG6000 crystals of each sample were growing until the minute of 35, liquid phase of the pure PEG6000 sample disappeared. With same phenomena, liquid phase of the samples that has fewer amount of ethanol gradually disappeared until the minute of 300, all of the samples were full of PEG6000 crystals. It was clear that ethanol had effect on nucleation and growth rate of PEG6000.

Due to the low dissolution of PEG6000 in SC-CO$_2$, The thermogravimetric analysis (TGA) could not detected the amount of PEG6000, Thus there was huge error of the amount of PEG6000 dissolved in SC-CO$_2$ that calculated by the amount of PEG6000 that remained in autoclave only.

Therefore, this study could conclude the potential of the effect of ethanol concentration, pre-expansion temperature and pre-expansion pressure on micronized PEG6000 as below.

Pre-expansion pressure ≈ Pre-expansion temperature < Ethanol concentration

4.3 Formulation of encapsulated particle of menthol and PEG6000

Due to limitation of PEG6000 dissolution in SC-CO$_2$, ethanol as co-solvent was necessary. Consideration from micronization of PEG6000, the amount of ethanol was necessary. The amount of ethanol was around 10, 30 wt% with pre-expansion pressure at 15, 20 MPa and pre-expansion temperature 313, 323 K. Consideration from micronization of menthol, menthol was well dissolved in SC-CO$_2$. After conducted preliminary experiments and then brought the sample to analyze by OM and SEM. There was difficult to separate menthol, PEG and the composite particle without morphology changing. Therefore, the low mass ratio between menthol and PEG6000 were chosen at 1:1 which low amount of menthol (2 grams) to avoid microniztion of menthol. Therefore, this work will investigate the suspected particles which should be the composite product by using scanning electron microscope (SEM). The results were shown in **Figure 4.28.**
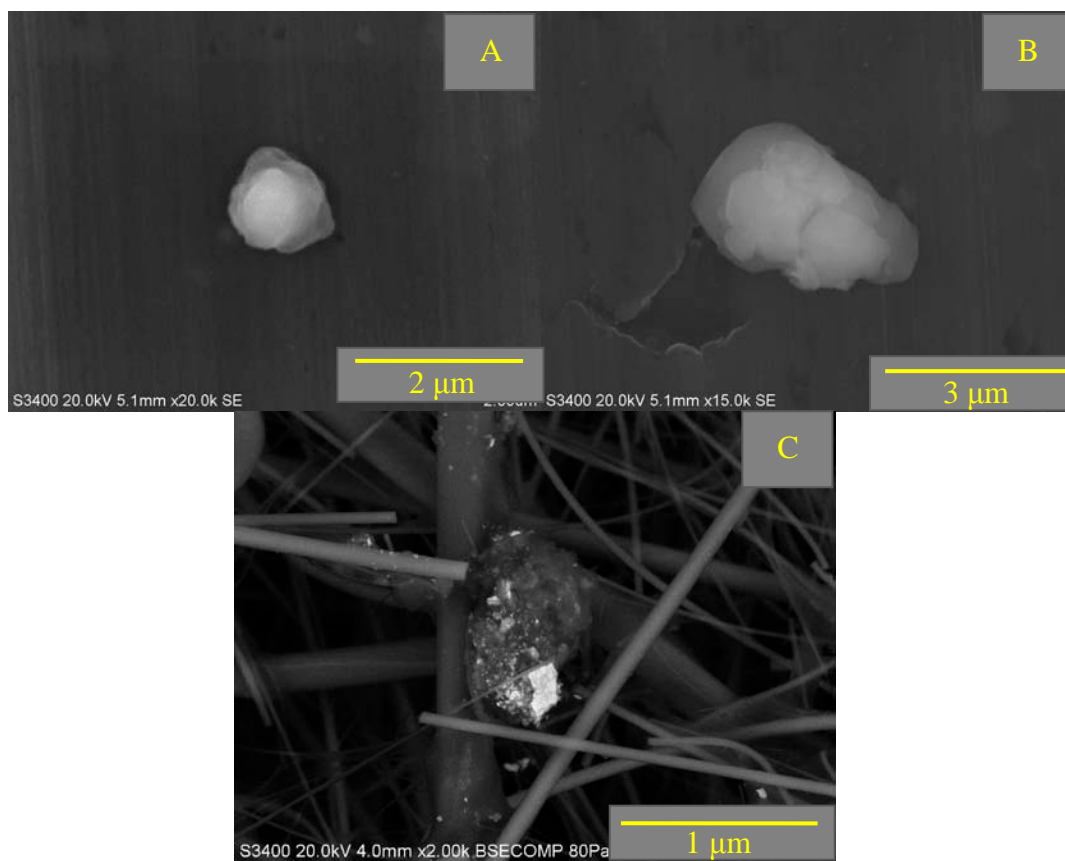
Figure 4.28 A) microencapsulation of the composite products, B) microsphere of the composite product and C) microsphere of the composite product on HEPA filter

As shown in **Figure 4.28**, the results showed that there were 2 kinds of the composite products, microsphere and microencapsulation. However, the composite products seemed to be microsphere from scanning electron microscope observation by random taking photograph and then compared with the images of menthol and PEG6000.

With the limitation of the amount of composite products and heat sensitivity of menthol, using Transmission electron microscopy (TEM) was unable to specify the type of matrix. However, the distinction of color (light gray and dark gray) might be identified that there were different matrix at the same electron intensity in SEM. Thus it was still doubtful that which matrix was menthol and PEG6000.

The particle size distribution, geometric mean size and standard deviation were shown in **Figure 4.29**
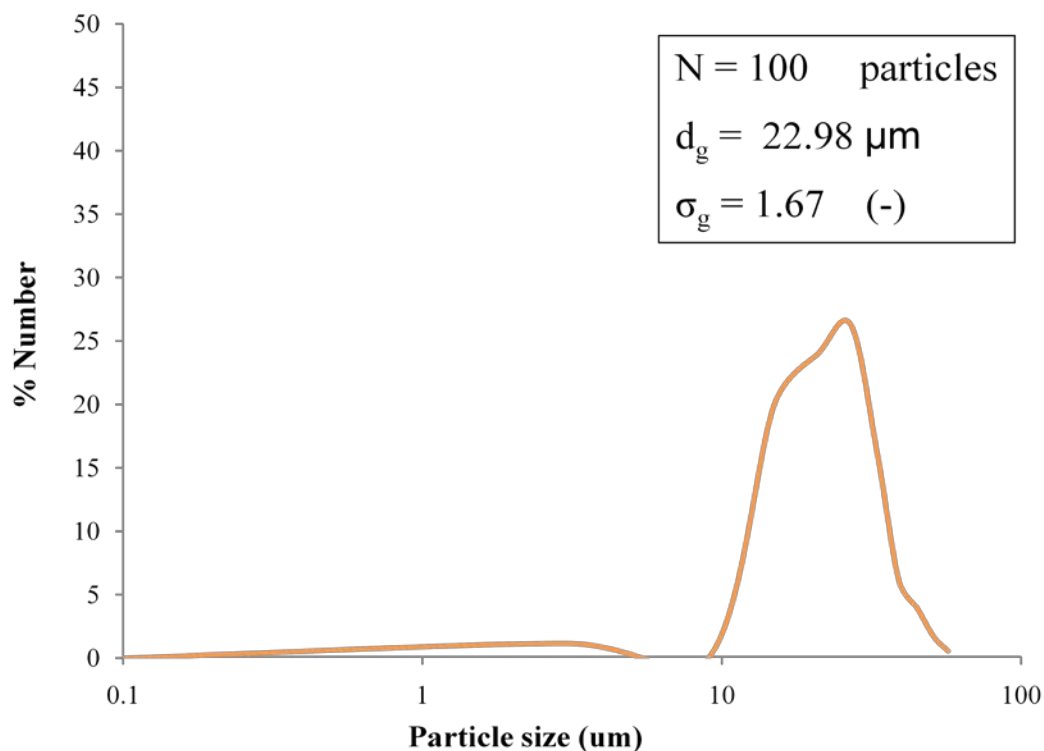
Figure 4.29 PSD of encapsulated particle at 323 K, 15 MPa and 15 wt% of ethanol concentration

From **Figure 4.29**, the obtained particle had geometric mean size around 23 μm and standard deviation around 1.67. The particle size was bigger than micronized menthol and micronized PEG6000. It might cause of the difference on particle formation. Due to PEG6000 had lower limitation to dissolve in SC-CO_2 than menthol, thus PEG6000 should precipitated first and encapsulated menthol inside. Menthol itself had high solubility in SC-CO_2, the smaller particle were obtained theoretically. However, there were different crystallographic faces of crystal that was a reason why the particle size was big in micrometer but the standard deviation was still narrow. It might be the affect of ethanol. Moreover, menthol should be affected on morphology and particle size

as well. To investigate the effect of menthol on nucleation and growth rate of the encapsulated particle. the set of crystallization experiments of menthol and PEG6000 system were carried out. Both of PEG6000 and menthol were liquid phase by heating with hot plate at 323 K and then titrate the solutions of PEG6000 and menthol with different concentration as shown in **Figure 4.30.**
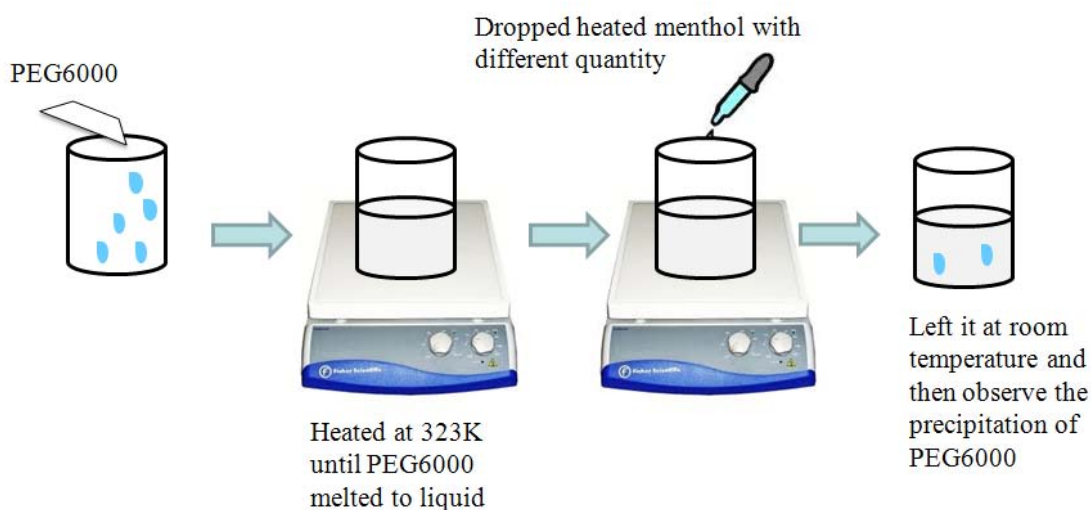
Figure 4.30 Preparation of PEG6000 and menthol crystallization in liquid phase

After finished preparation of solution, the experiment was observed the density of PEG6000 crystals in vivo by visual that was shown in **Figure 4.31.**
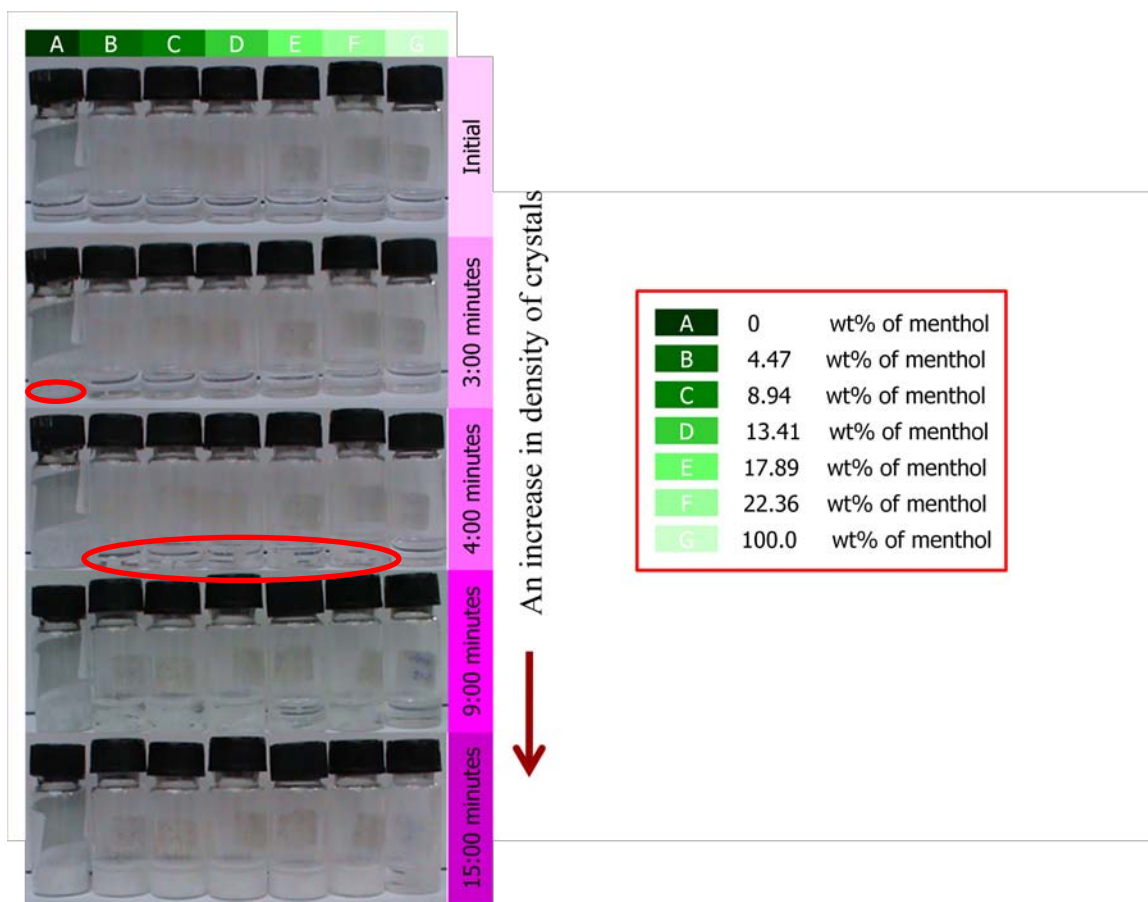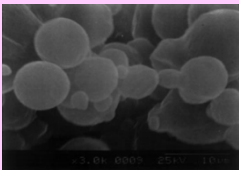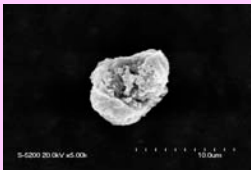
Figure 4.31 Crystallization of PEG6000 and menthol in liquid phase at different menthol concentration

As results from **Figure 4.31**, pure PEG6000 precipitated around the minute of 3:00 by visual and then at minute of 4:00 the PEG6000 crystals of sample B,C,B,E and F were precipitated after that PEG6000 crystal were growing until the minute of 15, liquid phase of the pure PEG6000 sample disappeared and there were some menthol crystals of sample G precipitated. It was clear that menthol had effect on nucleation and growth rate of PEG6000. It made the growth rate of PEG6000 slowly because they were different crystallographic faces of crystal. Therefore, menthol might be obstructed the growth sites of PEG6000. Thus the growth rate of PEG6000 crystal was slow. This might be a reason

why the encapsulated particle had a bigger particle size than original micronized PEG6000 and original micronized menthol.

This work also benchmarked against other work related encapsulation of any drug with PEG6000 via RESS-CO_2. The result was shown in **Table 4.1 .**

Table 4.1 Comparison of some parameters on encapsulated particle by using RESS-CO_2

	Matsuyama et al. (2000)	Matsuyama et al. (2002)	This work
Material	PEG6000+lipase	PEG6000+flavone	PEG6000+menthol
Type of encapsulated particles	Microencapsulation	Microencapsulation	Microspheres Microencapsulation
Particle size	9-62 µm	10-35 µm	0.5-60 µm
Diameter	Equivalent light-scattering diameter	Equivalent light-scattering diameter	Equivalent projected area diameter
Morphology	*Spherical*	Spherical	Almost circle

The results were different not too much. The particle size was same in range of micrometer. The different of process equipment might be a reason why morphology of this work was different from the other because during spraying, the equipment could not supplied ethanol into the autoclave. Therefore, almost of encapsulated product were precipitated in the autoclave due to solubility of PEG6000 dropping rapidly. Therefore, both experiments in **Part 4.2** and **Part 4.3**, there were a small amount of the product. A few particles could pass through the nozzle to collecting chamber.

To improve product yield of micronized PEG6000 and the encapsulated particles. This work also proposed a suggestion in **Part 5.4**.

CHAPTER V

CONCLUSION AND RECOMMENDATION

5.1 Conclusion

In this work, the fundamental knowledge about controlling morphology, particle size and particle size distribution were investigated through the RESS parameters and ethanol concentration. These parameters related to dissolution of menthol and PEG6000 in SC-CO_2. Menthol was a good material for the RESS process due to its high solubility in SC-CO_2. On the other hand, the limitation of PEG6000 dissolution led to problems for product analysis. Adding a limited amount of ethanol as a co-solvent proved to be insufficient, while adding a larger amount ethanol, may result product deformation due to the ethanol condensation. The suitable amount of ethanol should be determined similar to RESS parameters.

5.1.1 Micronization of menthol

Because of the high solubility of menthol in CO_2, this study was able to formulate micronized menthol by RESS-CO_2 in the micrometer range without using ethanol. However, ethanol could help to improve particle size distribution to obtain smaller particles with a narrow size distribution. Increasing the pre-expansion temperature should make the solution undergo a high degree of supersaturation. Thus the product should be smaller in size than with a higher temperature.

Regarding pressure, increasing pressure led to a high density of CO_2. This can help to attain high solubility of the menthol, but in our case, it led to low degree of supersaturation due to the menthol could dissolve in CO_2 completely. With no need to increase the solubility, a bigger size should be obtained; however, adding ethanol affected the nucleation and growth rate of menthol significantly. For this reason, the particle size was still small and particle size distribution was also narrow.

5.1.2 Micronization of PEG6000

The selection of PEG6000 as a coating material was beneficial as it is one of the base polymers used in pharmaceuticals. However, the limitation of PEG6000 dissolution resulted in obtaining an insufficient amount of the product. Thus it was difficult to get further analysis. With repeated experiments and analysis however, usable results were eventually achieved. The results were similar to that of the menthol. Thus the fundamentals of controlling particle size were obtained which were conducting the experiment at a high pre-expansion pressure (15, 20 MPa), high ethanol concentration (10%, 30%) and high pre-expansion temperature (313K, 323K).

5.1.3 Formation of encapsulated particle of menthol and PEG6000

As mentioned earlier, the high solubility of PEG6000 was necessary for the process. Conducting experiments, with a high ethanol concentration always resulted in product deformation. This could also have occurred during the spraying process. The product remained in the instrument even when trying to supply fresh CO_2. Although the amount of the product remained low, the study results, revealed the product tent to be microspheres; and though some of microcapsule were produced, it was difficult to find them by SEM.

5.2 Recommendation for future work

This technique should be improved regarding the method to achieve high solubility for poor CO_2 soluble material like PEG6000. Installation of solvent mixing chamber and an agitator should be tried. The efficiency of the spraying zone is also significant for use with a high concentration of co-solvents like ethanol to prevent product deformation caused by ethanol condensation. Finally, it will be great if the instrument could be constructed view cell to observe the phase behavior of the system in order to ensure the results of the experiments and obtain greater solubility data in SC-CO_2. The recommended process is shown in **Figure 5.1.**
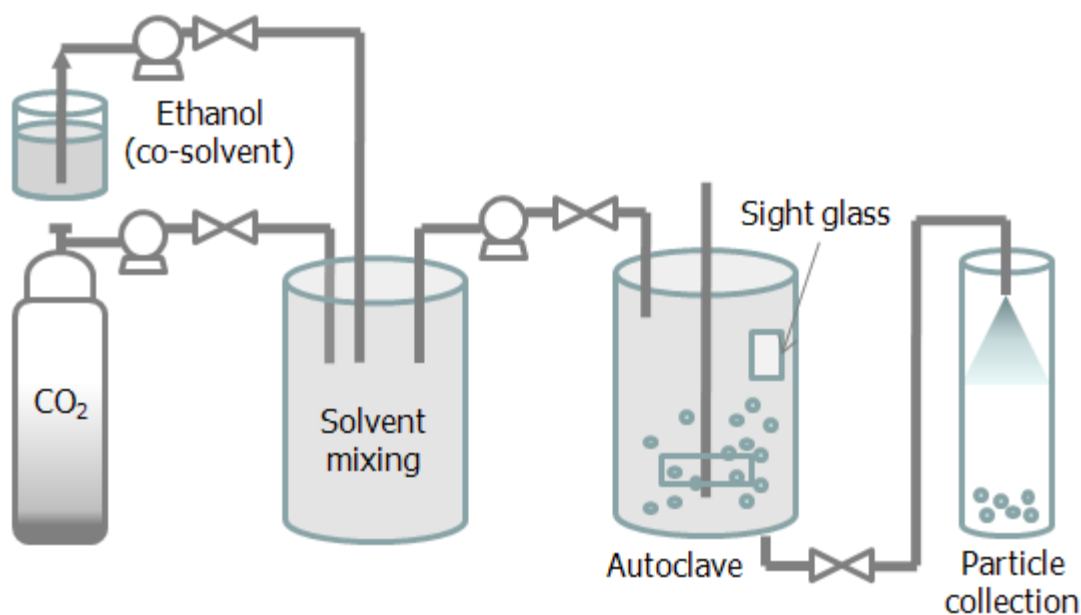
Figure 5.1 Recommended process for future study

REFFERENCES

Brahrami, M., Ranjbarian, S. Production of micro- and nano-composite particles by supercritical carbon dioxide. The journal of supercritical fluids 40 (2007) : 263-283.

Benjapol Kongsombut. Polymer coating of fine particles using supercritical carbon dioxide technology with ethanol cosolvent. Doctoral dissertation, Department of chemical engineering Faculty of Engineering Chulalongkorn University 2009

Brennecke, J. F., Eckert, C. A. Phase equilibria for supercritical fluid process design. AIChE J. 35 (1989) : 1409-1427.

Brunner, G. H. Supercritical Fluids as Solvents and Reaction Media. Hamburg : Elsevier Science & Technology Books, 2004

Chattopadhyay, P., Gupta, R.B. Production of griseofulvin nanoparticles using supercritical CO_2 antisolvent with enhanced mass transfer. International Journal of Pharmaceutics 228 (2001) 19-31.

Charoenchaitrakool, M., Dehghani, F., Foster, R., Chan H. K. Micronization by rapid expansion of supercritical solutions to enhance the dissolution rates of poorly water-soluble pharmaceuticals. Ind. Eng. Chem. RES 39(2000) : 4794-4802.

Colussi, S., Elvassore, N., Kikic, I. A comparison between semi-empirical and molecular-based equations of state for describing the thermodynamic of supercritical micronization process. Journal of Supercritical Fluids 38 (2006) : 1097 – 1104.

Davey, R.J. Industrial crystallization 78, 169. North Holland. Amsterdam, 1979.

D. Randolph A. Theory of particulate process analysis and techniques of continuous crystallization. Academic press, San Diego, 1988.

Debenetti, P.G., Tom, J.W., Yeo, S.-D. Rapid Expansion of Supercritical Solutions (RESS): Fundamentals and Applications. Fluid Phase Equilibrium 82 (1993) : 311-321.

Domingo, C., Berends, E., van Rosmalen, G. M. Precipitation of ultrafine organic crystals from the rapid expansion of supercritical solutions over a capillary and frit nozzle. Journal of Supercritical Fluids 10 (1997) : 39-55.

Food-INFO. [Online]. Available from: http://www.food-info.net/uk/qa/qa-fi71.htm [2554, June]

Gong, K., Rehman I.U., Darr, J.A. Synthesis of poly(sebacic anhydride)-indomethacin controlled release composites via supercritical carbon dioxide assisted impregnation. International Journal of Pharmaceutics 338 (2007) : 191-197.

Guney-Altay, Ozge., Levit, N., Pestov, D., Tepper, G. Precipitation of nanocomposite particles from a multi-component, rapidly expanding supercritical solution. Journal of Supercritical Fluids 37 (2006) : 229-241.

Gupta, R. B., Shim, J. J. Solubility in Supercritical Carbon Dioxide. Boca Raton : CRC Press, 2007.

Huang, Z., Sun, G., Chiew, Y. C., Kawi, S. Formation of ultrafine aspirin particles through rapid expansion of supercritical solution (RESS). Powder technology 160 (2005) : 127-134.

Hyatt, J. A., Liquid and supercritical carbon dioxide as organic solvents. J. Org Chem. 49 (1984) : 5097-5101.

Ikushima, Y., Saito, N Arai, M. Arai K. Solvent polarity parameters of supercritical carbon dioxide as measured by infrared spectroscopy. Bull Chem. Soc. Jpn. 64 (1991) : 2224-2229.

Jennings, D. W., Lee R. J., Teja, A. S. Vapor-liquid equilibria in the carbon dioxide + ethanol and carbon dioxide + 1-butanol systems. Journal of Chemical Engineer Data 36 (1991) : 303-307.

Joung, S. N., Yoo, C. W., Shin, H. Y. Kim, S. Y., Yoo K. P., Lee, C. Huh, W. S. Measurements and correlation of high-pressure VLE of binary CO_2-alcohol systems (methanol, ethanol, 2-methoxyethanol and 2-ethoxyethanol) Fluid phase Equilibria 185 (2001) : 219-230.

Jung, J., Perrut, M. Particle design using supercritical fluids: Literature and patent survey. The journal of supercritical fluids 20 (2001) : 179-219.

Kerč, J., Micronization of drugs using supercritical carbon dioxide. International journal of pharmaceutics 182 (1999) : 33-39.

Kiran, E., Xiong, Y., Zhuang. W. Modeling polyethylene solutions in near and supercritical fluids using the Sanchez-Lacombe model. J. Supercritical Fluids 6 (1993) : 193-203.

Knez, Ž., Weidner, E. Particles formation and particle design using supercritical fluids. Current Opinion in solid state and material science 7 (2003) : 353-361.

Li, G., Gunkel, F. Wang, J., Park C. B., Alstädt, V. Solubility measurements of N_2 and CO_2 in polypropylene and ethane/octane copolymer. J. Appl. Polym, Sci. 103 (2007) : 2945-2953.

Liu, G., Nagahama, K. Application of rapid expansion in the crystalline separation. Ind. Eng. Chem. Res. 35(1996) : 4626-4634.

Martín, A., Cocero M.J. Micronization processes with supercritical fluids: Fundamentals and mechanisms. Advanced Drug Delivery Reviews 60 (2008) : 339-350.

Matsuyama, K., Mishima, K., Hayashi, K., Matsuyama, H. Microencapsulation of TiO_2 nanoparticles with polymer by rapid expansion of supercritical solution. Journal of Nanoparticle Research 5 (2003) : 87-95.

Matsuyama K., Mishima, K., Hayashi, K., Ishikawa, H., Matsuyama H., Harada, T. Formation of microcapsules of medicines by the rapid expansion of a supercritical solution with a nonsolvent. Journal of Applied Polymer Science 89 (2003) : 742-752.

Matsuyama, K., Mishima, K. Phase behavior of CO_2 + polyethylene glycol + ethanol at pressure up to 20 MPa. Fluid Phase Equilibrium 249 (2006) : 173-178.

Mchugh, M. and Krukonis, V. J. Supercritical Fluid Extraction. Boston : Butterworth-Heinemann, 1994.

Mishima K., Tokuyasu, T., Matsuyama K., Komotita, N., Enjoji, T., Nagatani, M. Solubility of polymer in the mixtures containing supercritical carbon dioxide and antisolvent. Fluid Phase Equilibrium 144 (1998) : 299-305.

Mishima K., Matsuyama K., Nagatani, M. Solubilities of poly(ethylene glycol)s in the mixtures of supercritical carbon dioxide and cosolvent. Fluid Phase Equilibrium 161 (1999) : 315-324.

Mishima K., Matsuyama K., Tanabe D., Yamauchi, S. Microencapsulation of Proteins by Rapid Expansionof Supercritical Solution with a Nonsolvent. AIChE J. 46 (2000) : 857-865.

Mishima, K. Biodegradable particle formation for drug and gene delivery using supercritical fluid and dense gas. Advanced Drug Delivery Reviews 60 (2008) : 411-432.

Menthol cigarettes no harzard to smoking [Online] Available form: http://www.cigarettesflavours.com/cigarettes-flavors/menthol-cigarettes-no-hazard-to-smoking/ [2554, June].

Moribe, K., Tozuka, Y., Yamamoto, K. Supercritical carbon dioxide processing of active pharmaceutical ingredients for polymorphic control and for complex formation. Advanced Drug Delivery Reviews 60 (2008) : 328-338.

Pöhler, H., Kiran, E. Volumetric properties of carbon dioxide + ethanol at high pressures. J. Chem. Eng. Data. 42 (1997) : 384-388.

Prausnitz, J. M., Lichtenthaler, R. N. Azevedo, E. G. Molecular Thermodynamics of Fluid Phase Equilibria. 2nd ed. New Jersey : Prentice-Hall, 1986.

Rantakyla, M. Particle Production by Supercritical Antisolvent Processing Techniques. PhD Thesis Department of Chemical Technology Helsinki University of Technology, 2004.

Reverchon, E., Adani, R. Nanomaterial and supercritical fluids: Review. The journal of supercritical fluids 37 (2006) : 1-22.

Ribeiro Dos Santos, I., Richard, J., Pech, B., Thies, C., Benoit, J.P. Microencapsulation of protein particles within lipids using a novel supercritical fluid process. International Journal of Pharmaceutics 242 (2002) : 69-78.

Sanchez I. C., Lacombe, R. H., Statistical Thermodynamics of Polymer Solutions. Macromolecules November-December 11 (1978) : 1145-1156.

Sarah, S. L., Veatch, L. Keller S. L. Separation of liquid phases in giant vesicles of ternary mixtures of phospholipids and cholesterol. Biophys. J. 85 (2003) : 3074-3083.

Shekunov, B. Y. Hanna, M., York P. Crystallization process in turbulent supercritical flows. J. Cryst. Growth. 198/199 (1999) : 1345-1351.

Smith, R. D. Kalinoski, H. T. Udseth, H. R. Fundamentals and practice of supercritical fluid chromatography-mass spectrometry. Mass Spectum. Rev.6 (1987) : 445-496.

Sovová, H., Stateva, R. P., Galushko, A. A. High-pressure equilibrium of menthol+CO_2, J. Supercritical Fluids 41 (2007) : 1-9.

Stahl, E. Schüutz, E., Mangold, H. K. Extraction of seed oils with liquid and supercritical carbon dioxide. Journal of Agricultural and Food Chemistry. 28 (1980) : 1153-1159.

Suzuki, K., Sue H. Isothermal vapor-liquid equilibrium data for binary systems at high pressures : carbon dioxide-methanol, carbon dioxide-ethanol, carbon dioxide-1-propanol, methane-ethanol, methane-propanol, ethane-ethanol, ethane-1-propanol systems. J. Chem. Eng. Data. 35 (1990) 63-66.

Tandya, A., Mammucari R,. Dehgani, F., Foster, N. R., Dense gas processing of polymetric controlled release formulations. International Journal of Pharmaceutics 328 (2007) : 1-11.

Taylor, T. L. Supercritical fluid extraction. New York : John Wiley, 1996.

Thakur, R., Gupta, R. B. Formation of phenytoin nanoparticles using rapid expansion of supercritical solution with solid co-solvent (RESS-SC) process. International Journal of Pharmaceutics 308(2006) : 190 - 199.

Tsumi, A., Ikeda, M., Chen, W., and Iwatsuki, J. A nano-coating process by the rapid expansion of supercritical suspensions in impinging stream reactor, Powder Technology 138 (2003) : 211-215.

Türk, M. Formation of small organic particles by RESS : experimental and theoretical investigations. Journal of Supercritical Fluids 15 (1999) : 79-89.

Türk, M. Manufacture of submicron drug particles with enhanced dissolution behavior by rapid expansion processes. Journal of Supercritical Fluids 47 (2009) : 537-545.

Weidner, E., Wiesmet, V., Knez, Ž. Škerget M. Phase equilibrium (solid-liquid-gas) in polyethyleneglycol-carbon dioxide systems. Journal of Supercritical Fluids 10 (1997) : 139-147.

Werling, J. O., Debenedetti, P. G. Numerical modeling of mass transfer in the supercritical antisolvent process. J. Supercrit. Fluids. 16 (1999) : 167 – 181.

Xiong, Y., Kiran E. High-pressure phase-behavior in polyethylene n-butane binary and polyethylene n-butane CO_2 ternary-systems. Journal of Applied Polymer Science 53 (1994) : 1179-1190.

Yasuji, T., Takeuchi H., Kawashima, Y. Particle design of poorly water-soluble drug substances using supercritical fluid technologies. Advanced Drug Delivery Reviews 60 (2008) : 388-398.

Yeo, S., Kiran, E. Formation of polymer particles with supercritical fluids: A review. Journal of Supercritical Fluids 34 (2005) : 287–308.

Yoon, J. H., Lee H. High pressure vapor liquid equilibria fro cabon dioxide + methanol, carbon dioxide + ethanol, and carbon dioxide + methanol + ethanol. J. Chem. Eng. Data. 38 (1993) : 53-55.

Zúñiga-Moreno, A., Galicia-Luna, L. A. Compressed liquid densities of carbon dioxide + ethanol mixtures at four compositions via a vibrating tube densimeter up to 363 K and 25 MPa. J. Chem. Eng. Data. 47 (2002) : 149-154.

APPENDICES

APPENDIX A

CALCULATION OF THE AMOUNT OF PRODUCT OR RESIDUE BY THERMOGRAVIMETRIC ANALYSIS (TGA)

Regarding to %yield calculation, there were 2 places of sampling positions;

I) Inside collecting chamber (including HEPA filter)

II) Inside the autoclave

The amount of product was the first one and the second one was residue remaining inside autoclave. Because the product and residue was dissolved in solvent (using THF in case of menthol and using water in case of PEG6000), the total weight of sample had to be noted. Therefore, purity determining was necessary for calculation to find the whole amount of product or residue. The amount of product or residue can determine from TGA graph, for example;
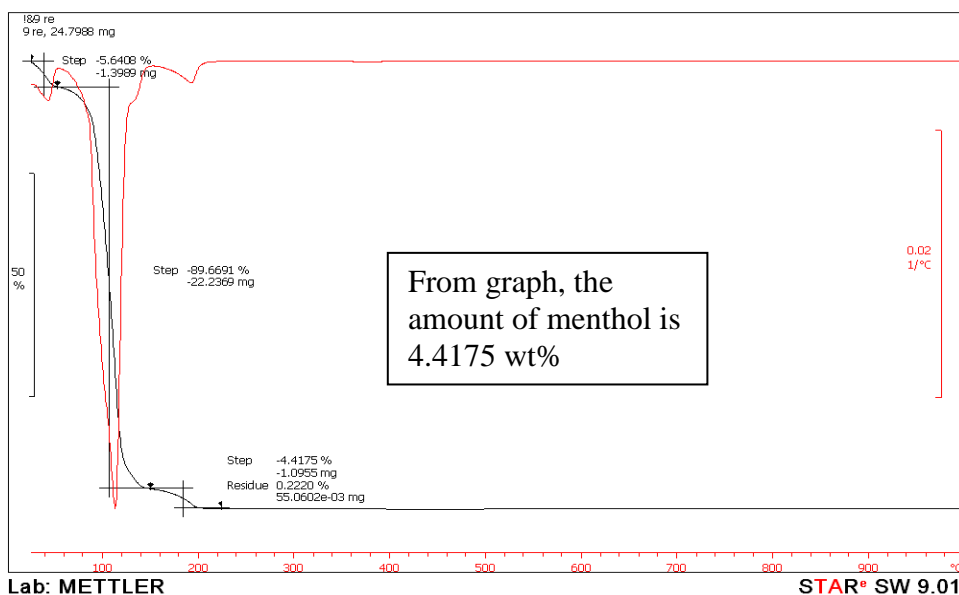

Figure A1 TGA graph of residue menthol at 303 K, 10 MPa and 10 wt% of ethanol concentration

Total amount of menthol that put in autoclave   4.17   g

This experiment used THF as solvent   30   ml

The total amount of sample is   26.42   g (including solvent)

From TGA graph, there was menthol $= 26.42 \times \frac{4.4175}{100} = 1.167\ g$

Therefore the amount of residue around   1.167 g

Converted to weight percent $= \frac{1.167}{4.17} \times 100 = 27.98\ wt\%$

Therefore, there was residue in autoclave 27.98 wt%

APPENDIX B

Publications

Journal

Publications Co-Authored by N. Suankaew:

Kongsombut, B., Tsutsumi, A. **Suankaew, N.**, Charinpanitkul, T. Encapsulation of SiO2 and TiO2 fine powders with poly(D,L-lactic-co-glycolic acid) by rapid expansion of supercritical CO_2 incorporated with ethanol cosolvent. Ind. Eng. Chem. Res., 48 (2009) : 11230-11235

International Conference Proceedings by N. Suankaew:

Suankaew N., Soottitantawat, A., Kongsombut, B., Matsumura, Y., Ruktanonchai, U.R., Sramala, I., Charinpanitkul, T. Micronization of menthol using rapid expansion of supercritical carbon dioxide. Proceedings of the 17th Regional Symposium on Chemical Engineering (RSCE2010), Queen Sirikit National Conventional Center, Bangkok, Thailand, November 22-23, 2010 : MSE 731.

VITA

Mr. Nara Suankaew was born in Angthong, Thailand on August 28, 1983. He studied in secondary educations at Angthong Pattamarojvitayakom School, Angthong. In 2006, he graduated Bachelor Degree of Engineering (Chemical Engineering) from King Mongkut's Institute of Technology Ladkrabang. After that, he continued to study in Master degree in Center of Excellence in Particle Technology at Department of Chemical Engineering, Faculty of Engineering, Chulalongkorn University.